Southeastern Geology: Volume 32, No. 1 July 1991

Edited by: S. Duncan Heron, Jr.

Abstract

Academic journal published quarterly by the Department of Geology, Duke University.

SOUTHEASTERN GEOLOGY

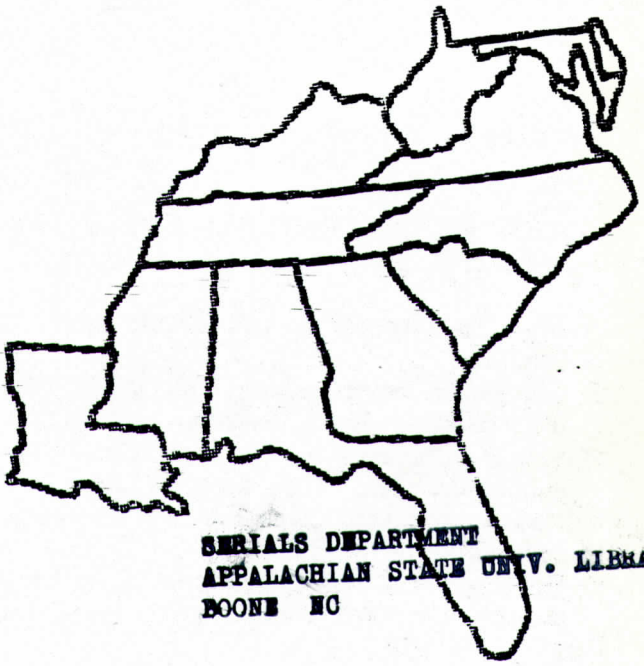

PUBLISHED AT DUKE UNIVERSITY DURHAM, NORTH CAROLINA

VOL. 32, NO. 1 JULY 1991

SOUTHEASTERN GEOLOGY

PUBLISHED

AT

DUKE UNIVERSITY

Editor in Chief:
S. Duncan Heron, Jr.

Managing Editor:
James W. Clarke

This journal publishes the results of original research on all phases of geology, geophysics and geochemistry as related to the Southeast. Send manuscripts to S. DUNCAN HERON, JR., DUKE UNIVERSITY, DEPARTMENT OF GEOLOGY, OLD CHEMISTRY BUILDING, DURHAM, NORTH CAROLINA 27706. Observe the following:

1) Type the manuscript with double space lines and submit in duplicate.
2) Cite references and prepare bibliographic lists in accordance with the method found within the pages of this journal.
3) Submit line drawings and complex tables reduced to final publication size (no bigger than 8 x 5 1/8 inches).
4) Make certain that all photographs are sharp, clear, and of good contrast.
5) Stratigraphic terminology should abide by the North American Stratigraphic Code (Am. Assoc. Petroleum Geologists Bulletin, v. 67, p. 841-875).

Subscriptions to *Southeastern Geology* are $12.00 per volume (US and Canada), $16.00 per volume (foreign). Inquires should be sent to: SOUTHEASTERN GEOLOGY, DUKE UNIVERSITY, DEPARTMENT OF GEOLOGY, OLD CHEMISTRY BUILDING, DURHAM, NORTH CAROLINA 27706. Make checks payable to: *Southeastern Geology*.

ISSN 0038-3678

SOUTHEASTERN GEOLOGY

Table of Contents

Vol. 32, No. 1

July 1991

MIDDLE EOCENE AND LATE OLIGOCENE ISOTOPIC DATES OF GLAUCONITIC MICA FROM THE SANTEE RIVER AREA, SOUTH CAROLINA

W. BURLEIGH HARRIS
Department of Earth Sciences
University of North Carolina at Wilmington
Wilmington, NC 28403

PAUL D. FULLAGAR
Department of Geology
University of North Carolina at Chapel Hill
Chapel Hill, North Carolina 27599

ABSTRACT

Evolved (high-potassium) glauconitic micas from the stratotype of the Warley Hill Formation (calcareous nannofossil zone NP15), the Chapel Branch Member of the Santee Limestone (calcareous nannofossil zones NP16-17), and the Ashley Formation of the Cooper Group (calcareous nannofossil zone NP24), yield Rb-Sr isochron dates of 41.6 ± 1.5 Ma, 40.4 ± 0.8 Ma, and 26.2 ± 1.2 Ma, respectively. Two glauconitic micas from the Warley Hill Formation yield an average conventional K-Ar date of 45.1 ± 1.7 Ma. The Rb-Sr date of the Warley Hill Formation is generally younger than the numerical limits that are assigned to the zone by recent time scales and is considered to be younger than deposition of the unit. The K-Ar date, which agrees with the limits of most time scales and other reported dates of equivalent sediments from the southeastern Atlantic and Gulf Coastal Plains, is considered to represent the time of deposition of the unit. The Rb-Sr 40.4 ± 0.8 Ma date of the Chapel Branch Member of the Santee Limestone agrees with the numerical limits placed on its assigned zone by most recent time scales, and with other dates reported for equivalent sediments in the southeastern Atlantic and Gulf Coastal Plains. It does not agree with a reported Rb-Sr glauconitic mica isochron date for the Santee Limestone of 36.7 ± 0.6 Ma from Berkeley County, South Carolina. This latter date is now considered to be too young. The 26.2 ± 1.2 Ma date for the Ashley Formation of the Cooper Group agrees with several numerical estimates that are placed on its assigned calcareous nannofossil zone by recent time scales. In the absence of complementary volcanic mineral dates, glauconitic mica dates are difficult to evaluate solely by their comparison to published time scales. This emphasizes that radiometric dates should be evaluated using their assigned analytical uncertainties plus the uncertainties of a unified stratigraphic framework rather than absolute values.

INTRODUCTION

The use of glauconite as a chronometer in time scale studies has divided most

geochronologists into two groups; those who are strong advocates of its use, and those who suggest that there are only a few cases where glauconite dates should be used, such as where they agree within their assigned analytical uncertainties with dates from coeval volcanic minerals. Odin (1982), Odin and Curry (1985), and Harris and Fullagar (1989) suggested that if very strict procedures are used to select glauconites (glauconitic micas) for dating, they can provide meaningful information for time scale studies. Obradovich (1964), Prothero and others (1982), and Berggren and others (1985) have strongly attacked the use of glauconites for time scale calibration and have generally ignored the results of K-Ar and Rb-Sr glauconite dates unless they agreed with dates from volcanic minerals.

Because of the ambiguous use of the term glauconite, Odin and Matter (1981) proposed the word glaucony as a facies name for authigenic green pelletal material with no specific mineralogy, and either glauconitic mica or glauconitic smectite, depending upon its clay mineralogy, for end-members of a specific mineral family. They suggested that only glauconitic mica which contains greater than 6 percent K_2O is useful in radiometric studies. In this paper we follow Odin and Matter (1981) and use the term glaucony for any green mineral with an unknown mineral composition, and the term glauconitic mica or glauconitic smectite for specific minerals.

Odin (1982) stressed that if the complete history of the glauconite sample is well-known, the geochronologist can decide before it is dated whether the sample will yield geologically accurate results. We have attempted (Harris, 1982; Harris and Fullagar, 1982; 1987; 1988; and Harris and others, 1984) to select only those samples with well-documented histories that meet Odin's (1982) mineralogical criteria, and also to exclude those that have undergone weathering or reworking. However, we have found that some glauconites meet selection criteria but yield geologically erroneous results (Santee Limestone data discussed herein and reported by Harris and others, 1984, and unpublished data) when their dates are compared to the numerical limits of published time scales. A better method of checking the geologic accuracy of glauconitic mica dates is to compare the dates to coeval volcanic dates; however, few comparative studies have been made (Obradovich, 1988). Harris and Fullagar (1989) compared glauconitic mica dates with dates from coeval volcanic minerals from the Castle Hayne Limestone and found that these results were in analytical agreement.

Obradovich (1988) suggested that some glauconitic micas dated by the Rb-Sr isochron method yield dates that approximate the time of deposition, but also indicated that "...only when all data are assembled and viewed in context of a single stratigraphic framework...does it become evident that some of the published Rb-Sr isochrons are clearly anomalous." This paper presents three new Rb-Sr isochron dates and one K-Ar date for Tertiary units from South Carolina, and discusses them within a single stratigraphic framework. From this analysis we show that some of these glauconitic mica dates seem to provide useful information for time scale calibration. Dates are reported for the middle Eocene Warley Hill Formation and Chapel Branch Member of the Santee Limestone, and the upper Oligocene Ashley Formation of the Cooper Group. The dates are also discussed within the context of other published dates for units in the southeastern Atlantic and Gulf Coastal Plains that can be assigned to the same biostratigraphic zones. In this paper, use of

Warley Hill Formation follows that of Nystrom and others (1989) and use of Santee Limestone follows that of Baum and others (1980).

GEOLOGIC SETTING

Warley Hill Formation

The Eocene Warley Hill Formation consists of green, quartzose and glauconitic non-calcareous sediments that are exposed in north-central and western Calhoun County and northwestern Orangeburg County, South Carolina (Nystrom and others, 1989). In the Upper Coastal Plain, the Warley Hill Formation disconformably overlies the lower middle Eocene Congaree Formation and disconformably underlies the upper middle Eocene McBean Formation. In the Lower Coastal Plain, the Warley Hill Formation overlies the Black Mingo Group and underlies the upper part of the Santee Limestone (*Cubitostrea sellaeformis*-bearing beds) of Baum and others (1980). Semi-consolidated gray-green, highly glauconitic bryozoan mudstone-packstone that contains *Cubitostrea lisbonensis* and underlies the Santee Limestone at Wilson's Landing, Berkeley County, is correlated to the Warley Hill Formation of the type area (Cooke and MacNeil, 1952; Nystrom and others, 1989). Harris and Fullagar (1987) reported a Rb-Sr glauconitic mica isochron date of 42.0 ± 0.5 Ma for sediments at Wilson's Landing and correlated the sediments to the type Warley Hill Formation in Calhoun County.

The Warley Hill Formation is correlated to sequence 1 of the Castle Hayne Limestone in North Carolina (Zullo and Harris, 1987), the lower Lisbon Formation of Alabama (Toulmin, 1977), the Winona Formation of Mississippi (Dockery, 1980), and the lower Weches Formation of Texas (Stenzel, 1949). It is considered to be middle middle Eocene in age (Cooke and MacNeil, 1952; Nystrom, 1987; Nystrom and others, 1989). Zullo and Harris (1987), who placed North Carolina Paleogene sediments in a coastal onlap framework and correlated the sediments to the Santee River area of South Carolina, assigned the Warley Hill Formation to the TA3.4 Cycle of Haq and others (1987).

Samples of the Warley Hill Formation were collected from the stratotype in Calhoun County along the south side of S. C. Highway 267, and an abandoned road located about 30 m south of the highway (Figure 1). Six size-fractions of glauconitic-mica from the stratotype were dated by the Rb-Sr model and isochron methods; one size fraction was dated by the conventional K-Ar technique. One sample from the abandoned road was also dated by the conventional K-Ar technique.

Chapel Branch Member of the Santee Limestone

The Chapel Branch Member of the Santee Limestone was named by Powell (1984) for soft foraminiferal wackestone exposed on the south shore of Lake Marion in Orangeburg County. The unit consists principally of micrite and foraminifers but contains various allochems including echinoid fragments, molluscs, ostracods and bryozoans. Willoughby (1989, personal communication) recognized calcareous glauconitic beds in the Chapel Branch Member in Orange-

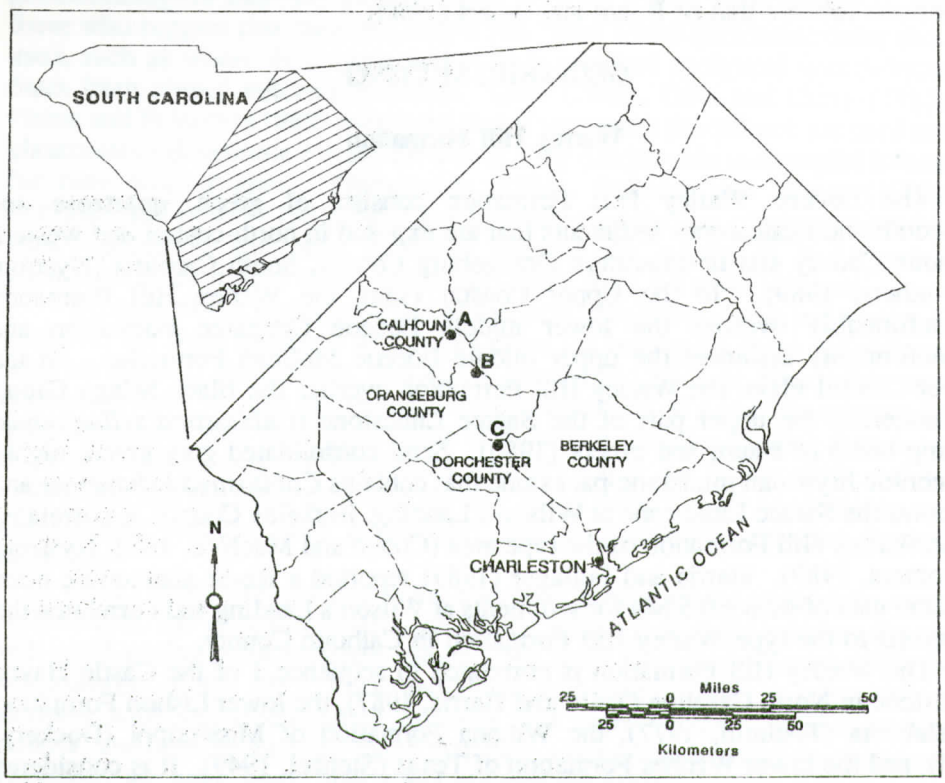

Figure 1. Source localities of glauconite-rich samples collected from Eocene and Oligocene units and dated in this study. A = locality in Warley Hill Formation, B = locality in Chapel Branch Member of the Santee Limestone, C = locality in Ashley Formation of the Cooper Group.

burg and Calhoun Counties. The Chapel Branch Member disconformably overlies the Warley Hill Formation and disconformably underlies the Harleyville Formation of the Cooper Group. Harris and others (1984) reported a Rb-Sr isochron date of 36.7 ± 0.6 Ma from beds at the Martin Marietta Quarry, Berkeley County, that are correlated to the Chapel Branch Member.

The Chapel Branch Member of the Santee Limestone contains the age diagnostic oyster *Cubitostrea sellaeformis* and echinoid *Protoscutella conradi* which allows correlation of the unit to the type Santee Limestone at Eutaw Springs, Orangeburg County, and to the upper Lisbon Formation of Alabama. It is considered to be late middle Eocene in age (Cooke and MacNeil, 1952; Nystrom, 1987; and Nystrom and others, 1989). Zullo and Harris (1987) assigned the *Cubitostrea sellaeformis*-bearing beds of the Santee Limestone to the TA 3.6/3.5 Cycles of Haq and others (1987).

A single sample of the Chapel Branch Member was collected in Santee State Park, Orangeburg County, about 100 m east of the boat ramp that occurs at the termination of S. C. Highway 82. This exposure has since been covered with rip-

rap and is no longer available for study; however, glauconitic sediments are also exposed along the shore of the lake just west of the boat ramp and probably represent the same unit (Willoughby, 1989, personal communication). Five size-fractions of glauconitic mica were dated by the Rb-Sr isochron and model dating methods.

Ashley Formation of the Cooper Group

Ward and others (1979) proposed the name Ashley Member of the Cooper Formation for calcareous very fine quartz sand that contains phosphate and mud in Dorchester County, South Carolina, and designated the section exposed at the Giant Quarry as a reference stratotype. Weems and Lemon (1984) raised the Ashley Member to formation rank and the Cooper Formation to group rank and mapped the general distribution of the unit in parts of Berkeley, Dorchester, and Charleston Counties (Weems and Lemon, 1984a; 1984b; 1988; 1989). The Ashley Formation disconformably overlies either the Eocene Parkers Ferry or Harleyville Formations of the Cooper Group, and is disconformably overlain by the Oligocene Chandler Bridge Formation.

Ward and others (1979) indicated that the lower part of the Ashley Formation at the Giant Quarry (bed D) contained planktic foraminifers indicative of zone P21 of late Oligocene age. Hazel and others (1977) identified the Ashley Formation in the Clubhouse Crossroads Core from near Charleston and assigned it to calcareous nannofossil Zone NP24 because of the overlapping ranges of *Helicopontosphaera* (=*Helicosphaera*) *recta* and *Pontosphaera clathrata* with *Helicopontosphaera compacta* and *Sphenolithus predistentus*; the latter calcareous nannofossils became extinct in zone NP24. Hazel and others (1977) also indicated that foraminifers, ostracodes, dinoflagellates and pollen indicate a late Oligocene age for the Ashley Formation. Weems and Lemon (1984a; 1984b; 1988; 1989) place the Ashley Formation in the late Oligocene. Harris and Zullo (in press) correlated the Ashley Formation to the TB1.1 coastal onlap cycle of Haq and others (1987) on the basis of faunal assemblages and regional stratigraphy.

One sample of the Ashley Formation was collected on the east wall of the Giant Quarry, Dorchester County, 15-20 cm above the lower contact with the Harleyville Formation (Figure 1). Five glauconitic mica concentrates of different size were dated by the Rb-Sr isochron and model dating methods.

PROCEDURES

General sample selection, analytical and laboratory procedures for glauconitic mica dating are given in Harris and Bottino (1974) and Harris and Fullagar (1989); specific procedures are given in Appendix 1.

RESULTS

Warley Hill Formation

Six glauconitic micas from the stratotype of the Warley Hill Formation yield

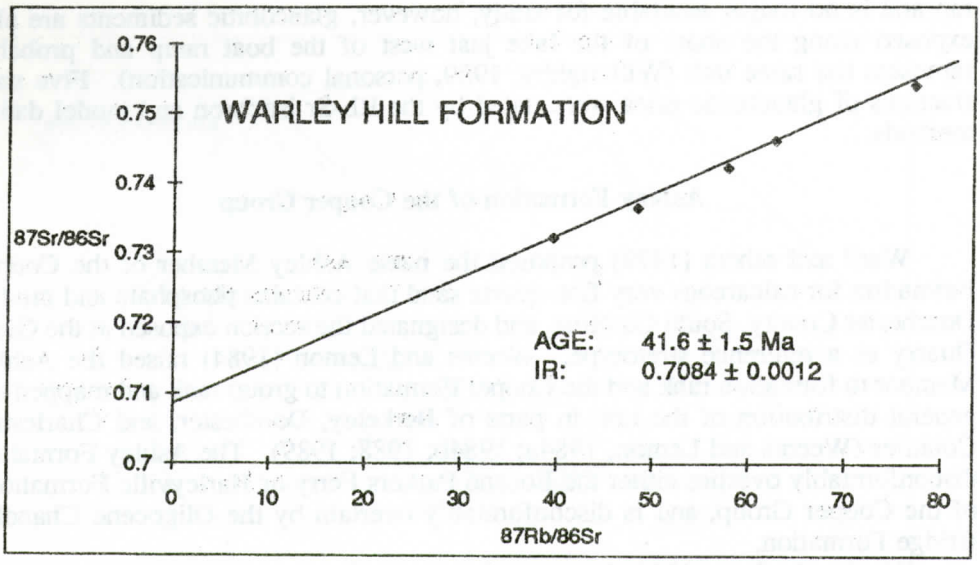

Figure 2. Rb-Sr isochron date of glauconitic mica from the middle middle Eocene Warley Hill Formation, Calhoun County, South Carolina. Size of data-points exceeds the one standard deviation errors in the $^{87}Rb/^{86}Sr$ and $^{87}Sr/^{86}Sr$ ratios. This is also the case in Figures 3 and 4.

a Rb-Sr isochron date of 38.4 ± 0.3 Ma with an initial $^{87}Sr/^{86}Sr$ ratio of 0.71077 ± 0.00025 and an MSWD of 12.3. However, one of these samples (H848-70) differs from the others by having an unusually low Sr content and a low model date (Table 1). These anomalous values could indicate that the glauconite has been altered; however, microscopic and x-ray diffraction analysis did not yield any signs of alteration of this sample. As this sample has a much higher $^{87}Sr/^{86}Sr$ ratio then the other five samples, it has the effect of controlling the slope of the isochron. Deletion of this sample results in a five-point isochron corresponding to a date of 41.6 ± 0.6 Ma with an initial $^{87}Sr/^{86}Sr$ ratio of 0.70838 ± 0.00050 and an MSWD of 5.3. As the MSWD value is still relatively high (indicating geological scatter in excess of analytical scatter), it is more appropriate to use the larger analytical errors provided by the York I version of York's (1969) regression calculation (41.6 ± 1.5 Ma; 0.7084 ± 0.0012). These are shown on Figure 2. Model dates for all six glauconitic micas range from 39.0 to 43.3 Ma and average 41.8 Ma; if sample H848- 70 is excluded, the model dates average 42.4 Ma (Table 1). Two samples yield conventional K-Ar dates of 46.6 ± 1.8 Ma (same location as Rb-Sr samples), and 43.5 ± 1.7 Ma (collected along abandoned road) and average 45.1 ± 1.7 Ma (Table 1). The 45.1 ± 1.7 Ma average K-Ar date is slightly older than the Rb-Sr isochron date shown in Figure 2, and the average of the Rb-Sr model dates.

In calculating conventional K-Ar dates, it is assumed that all of the non-radiogenic ^{40}Ar in the sample is of atmospheric origin. If this assumption is correct, then the atmospheric $^{40}Ar/^{36}Ar$ ratio of 295.5 can be used to determine the amount of non-radiogenic ^{40}Ar in the sample. However, it is well documented that

many minerals can contain extraneous Ar (see Faure, 1986, for summary). This Ar could have originated in the precursor of the mineral being studied (inherited Ar), or it could have been incorporated into the mineral by processes other than in-situ

Table 1. Rb-Sr and K-Ar data for the Warley Hill Formation, the Chapel Branch Member of the Santee Limestone, and the Ashley Formation of the Cooper Group.

Warley Hill Formation

Sample	Rb (ppm).	Sr (ppm)	$^{87}Rb/^{86}Sr$	$^{87}Sr/^{86}Sr$	Model Date (Ma)*
H847-40	239.6	11.10	62.66	0.74599	43.0 ± 0.6
H848-40	251.9	18.46	39.59	0.73213	43.5 ± 0.6
H848-60	246.1	12.35	57.85	0.74224	42.1 ± 0.6
H848-70	251.0	3.75	195.9	0.81626	39.0 ± 0.6
H848-80	251.3	9.46	77.23	0.75394	42.2 ± 0.6
H848-100	250.9	15.02	48.46	0.73642	41.8 ± 0.6

Sample	Mean Wt % K	$^{40}Ar^*$ (%)	$^{40}Ar^*$ (ppm)	Model Date (Ma)
H8725	6.102	41.4	0.01997	46.6 ± 1.8
H8726	6.150	53.5	0.01878	43.5 ± 1.7

Chapel Branch Member of the Santee Limestone

Sample	Rb (ppm)	Sr (ppm)	$^{87}Rb/^{86}Sr$	$^{87}Sr/^{86}Sr$	Model Date (Ma)*
H8732-40	244.7	6.85	104.00	0.76762	40.6 ± 0.6
H8732-60	246.4	6.18	116.02	0.77485	40.8 ± 0.6
H8732-70	248.9	5.56	130.5	0.78339	40.8 ± 0.6
H8732-80	249.2	4.83	150.4	0.79432	40.6 ± 0.6
H8732-100	249.4	6.41	113.25	0.77394	41.2 ± 0.6

*Model dates were calculated using an initial $^{87}Sr/^{86}Sr$ ratio of 0.70768 which is the value reported for middle Eocene seawater by Koepnick and others (1985).

Ashley Formation of the Cooper Group

Sample	Rb (ppm)	Sr (ppm)	$^{87}Rb/^{86}Sr$	$^{87}Sr/^{86}Sr$	Model Date (Ma)**
H8735-40	232.8	79.0	8.53	0.71147	28.2 ± 2.0
H8735-60	251.4	44.06	16.52	0.71487	29.1 ± 2.0
H8735-70	246.0	45.61	15.61	0.71402	26.9 ± 2.0
H8735-80	242.7	34.3	20.49	0.71600	27.3 ± 2.0
H8735-100	237.0	31.82	21.56	0.71623	26.7 ± 2.0

**Model dates were calculated using an initial $^{87}Sr/^{86}Sr$ ratio of 0.70805 which is the published seawater value for the upper Oligocene reported by Koepnick and others (1985).

decay of ^{40}K (excess Ar). The presence of extraneous Ar would cause the conventional K-Ar date to be too old. Several glauconite samples of Recent and Tertiary age have been found to have dates that are much too old, although the use of highly-evolved, K-rich glauconite grains usually avoids this problem (Odin and Fullagar, 1988). Because the Warley Hill glauconite grains are highly evolved and contain at least 6 percent K_2O, these criteria do not suggest the presence of extraneous Ar. However, the discrepancies between the two K-Ar dates, and between the Rb-Sr and K-Ar dates, suggest that we should consider the possible effects of extraneous Ar. Also, the two samples analyzed for K and Ar have relatively low radiogenic ^{40}Ar contents (41.4 and 53.5 percent); for such samples the assumptions employed in correcting for non-radiogenic ^{40}Ar are especially critical to the accuracy of the calculated K-Ar date.

If extraneous Ar is present, both samples that were analyzed to determine K-Ar dates could have the same date. If we assume this to be the case, and further assume that the samples contain extraneous Ar of the same composition (i.e., the same initial $^{40}Ar/^{36}Ar$ ratio), both the date and initial ratio can be calculated. The date obtained for both samples is 39.4 Ma, and their initial $^{40}Ar/^{36}Ar$ ratio is 328; obviously, a small quantity of extraneous ^{40}Ar can have a significant effect on a K-Ar date. For these values to be valid, approximately 10 percent of the ^{40}Ar in each sample (0.002-0.003 ppm ^{40}Ar) would have to be extraneous. Data in Odin and Fullagar (1988) indicate that some Recent glauconites contain ten-times this quantity of extraneous ^{40}Ar. It would seem worthwhile to further investigate the possible presence and effects of extraneous ^{40}Ar in glauconites. From this study we can only say that the discrepancies between the Warley Hill dates could be due to the presence of extraneous Ar.

Chapel Branch Member of the Santee Limestone

Five glauconitic micas from the Chapel Branch Member of the Santee Limestone yield a Rb-Sr isochron date of 40.4 ± 0.8 Ma with an initial $^{87}Sr/^{86}Sr$ ratio of 0.7084 ± 0.0014 and an MSWD of 1.5 (Figure 3). Model dates for these glauconitic micas range from 40.6 to 41.2 Ma and average 40.8 Ma (Table 1).

Ashley Formation of the Cooper Group

Five glauconitic micas from the Ashley Formation of the Cooper Group yield a Rb-Sr isochron date of 26.2 ± 1.2 Ma with an initial $^{87}Sr/^{86}Sr$ ratio of 0.70836 ± 0.00030 and an MSWD of 1.8 (Figure 4). Model dates for these glauconitic micas range from 26.8 to 29.1 Ma and average 27.7 Ma (Table 1).

DISCUSSION AND CONCLUSIONS

Glauconite dates and their geologic interpretation are replete with problems which may vary from sample to sample, and therefore, are difficult to assess. For a discussion of these problems see Obradovich (1988) and Harris and Fullagar (1989). We previously suggested that carefully selected and prepared glauconitic micas yield reliable Rb-Sr dates (Harris and Fullagar, 1982). However, unpub-

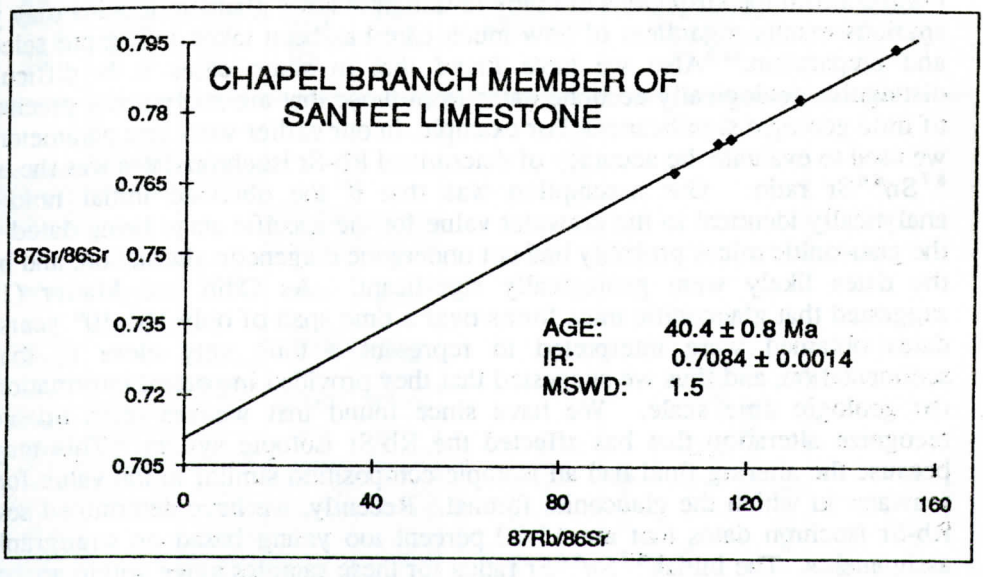

Figure 3. Rb-Sr isochron date of glauconitic mica from the upper middle Eocene Chapel Branch Member of the Santee Limestone, Orangeburg County, South Carolina.

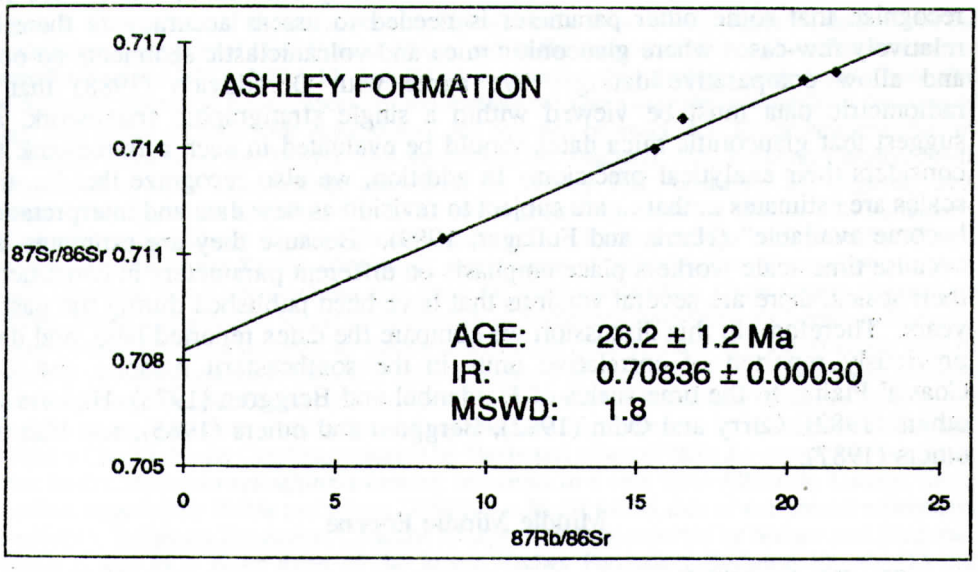

Figure 4. Rb-Sr isochron date of glauconitic mica from the lower upper Oligocene Ashley Formation of the Cooper Group, Dorchester County, South Carolina.

lished data from the Savannah River area of South Carolina and the Gulf Coastal Plain confirm the suspicions of many investigators that glauconitic mica may yield spurious results regardless of how much care has been taken in sample selection and preparation. Also we have found that in some cases it is difficult to distinguish geologically accurate dates from those that are analytically precise but of little geologic significance. For example, in our earlier work one parameter that we used to evaluate the accuracy of determined Rb-Sr isochron dates was the initial $^{87}Sr/^{86}Sr$ ratio. Our assumption was that if the obtained initial ratio was analytically identical to the seawater value for the specific stage being dated, then the glauconitic micas probably had not undergone diagenetic alternation, and hence the dates likely were geologically significant. As Odin and Matter (1981) suggested that glauconitic mica forms over a time span of only 10^5-10^6 years, the dates obtained were interpreted to represent a time very close to that of sedimentation, and thus we suggested that they provided important information for the geologic time scale. We have since found that we are often unable to recognize alteration that has affected the Rb-Sr isotopic system. This may be because the altering fluid had an isotopic composition similar to the value for the seawater in which the glauconite formed. Recently, we have determined several Rb-Sr isochron dates that are 15-20 percent too young based on stratigraphical assignments. The initial $^{87}Sr/^{86}Sr$ ratios for these samples agree within analytical uncertainty to the suggested seawater value for the time of their formation.

We previously suggested that if isotopic dates become younger as the units become geologically younger, agree with other reported dates from correlative units, and are consistent with an acceptable geologic time scale, they are accurate. With additional studies, we have discovered clearly anomalous dates. We now recognize that some other parameter is needed to assess accuracy as there are relatively few cases where glauconitic mica and volcaniclastic sediments co-occur and allow comparative dating. We agree with Obradovich (1988) that all radiometric data must be viewed within a single stratigraphic framework, and suggest that glauconitic mica dates should be evaluated in such a framework that considers their analytical precision. In addition, we also recognize that "... time scales are estimates ... that ... are subject to revision as new data and interpretations become available" (Harris and Fullagar, 1989). Because they are estimates, and because time scale workers place emphasis on different parameters in constructing their scales, there are several versions that have been published during the past 10 years. Therefore, in this discussion we compare the dates reported here, and dates previously reported of correlative units in the southeastern Atlantic and Gulf Coastal Plains, to the time scales of Hardenbol and Berggren (1978), Harland and others (1982), Curry and Odin (1982), Berggren and others (1985), and Haq and others (1987).

Middle Middle Eocene

The Warley Hill Formation is middle middle Eocene and in the Santee River area of South Carolina, is correlated to units that contain *Cubitostrea lisbonensis*. This establishes correlation of the unit to the lower Lisbon Formation of Alabama, and sequence 1 of the Castle Hayne Limestone in North Carolina. The lower

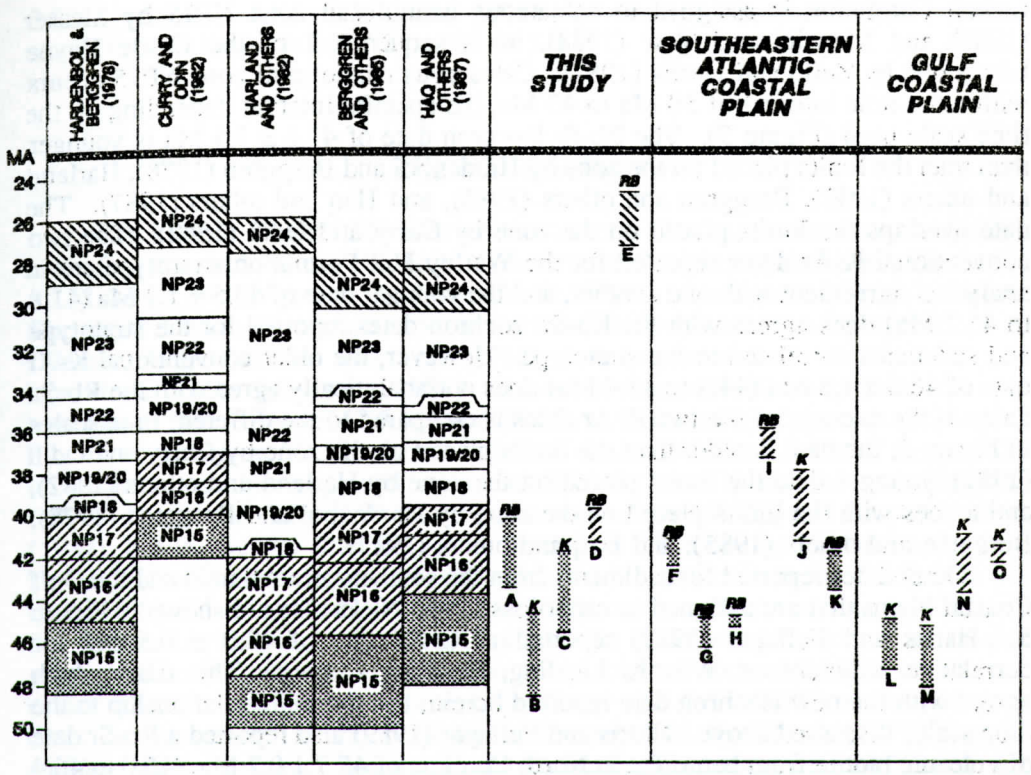

Figure 5. Comparison of the dates reported in this study to previously reported dates from the southeastern Atlantic and Gulf Coastal Plains, and to the numerical ranges placed on calcareous nannofossil zones NP15, NP16-17, and NP24 in several recent geologic time scales. Note that the assigned numerical limits placed on the nannofossil zones are interpolated from the ages of stage boundaries on each time scale shown and may not be exact. A = Rb-Sr isochron date of glauconitic mica from the Warley Hill Formation, SC Highway 267, Calhoun County, South Carolina; B = K-Ar conventional date from the Warley Hill Formation, SC Highway 267, Calhoun County, South Carolina; C = K-Ar conventional date from the Warley Hill Formation, abandoned road, Calhoun County, South Carolina; D = Rb-Sr isochron date from the Chapel Branch Member of the Santee Limestone, south shore of Lake Marion, Orangeburg County, South Carolina; E = Rb-Sr isochron date from the Ashley Formation, Giant Quarry, Dorchester County, South Carolina; F= Rb-Sr isochron date of sediments from Wilson's Landing, Berkeley County, South Carolina, reported by Harris and Fullagar (1987); G and H = Rb-Sr model date of bentonite (G) and glauconitic mica (H) from sequence 1 of the Castle Hayne Limestone, Billy B. Fussell Quarry, Duplin County, North Carolina, reported by Harris and Fullagar (1989); I = Rb-Sr isochron date from *Cubitostrea sellaeformis*-bearing sediments of the Santee Limestone, Berkeley County, South Carolina, reported by Harris and others (1984); J = average of two K-Ar dates from *Cubitostrea sellaeformis*-bearing sediments in a core from Allendale County, South Carolina, reported by Harris and others (1990); K = Rb-Sr model date of calcareous nannofossil zone NP15, Tallahatta Formation, Choctaw County, Alabama, reported by Siesser and Fitzgerald (1985); L and M = K-Ar dates of the lower Weches Formation, Burleson County (L) and Nacogdoches County (M), Texas, reported by Ghosh (1973); N and O = K-Ar dates of bentonite from the Landrum Member of the Cook Mountain Formation, Houston County, Texas, reported by Ghosh (1973) and by Obradovich (1988), respectively. Note that RB = Rb-Sr date and K = K-Ar date.

Lisbon Formation is assigned to calcareous nannofossil zone NP15 by Siesser (1983) and Mancini and Tew (1988), as is sequence 1 of the Castle Hayne Limestone by Zullo and Harris (1987). Calcareous nannofossil zone NP15 occurs within the time interval of 50 Ma to 40 Ma, the specific interval depending on the time scale used (Figure 5). The Rb-Sr isochron date of 41.6 ± 1.5 Ma is younger than than the limits placed on the zone by Hardenbol and Berggren (1978), Harland and others (1982), Berggren and others (1985), and Haq and others (1987). The date overlaps the limits placed on the zone by Curry and Odin (1982). The two conventional K-Ar dates reported for the Warley Hill Formation stratotype are in analytical agreement with one another, and the younger date of 43.5 ± 1.7 Ma (41.8 to 45.2 Ma) does agrees with the Rb-Sr isochron dates reported for the stratotype and sediments correlated to the stratotype. However, the older conventional K-Ar date of 46.6 ± 1.8 Ma (44.8 to 48.4 Ma) does not analytically agree with the Rb-Sr date. If the average of the two K-Ar dates is compared to the different time scales in Figure 5, the date is older than the limits placed on the zone by Curry and Odin (1982), younger than the limits placed on the zone by Harland and others (1982), and agrees with the limits placed on the zone by Hardenbol and Berggren (1978), Berggren and others (1985), and Haq and others (1987).

Other dates reported for sediments from the southeastern Atlantic and the Gulf Coastal Plains that are assigned to nannofossil zone NP15 also are shown in Figure 5. Harris and Fullagar (1987) reported a Rb-Sr date of 42.0 ± 0.5 Ma for correlative sediments at Wilsons Landing, Berkeley County. This date, which agrees with the new isochron date reported herein, has the same relationship to the time scales discussed above. Harris and Fullagar (1989) also reported a Rb-Sr date of volcanic biotite from bentonite in North Carolina of 45.7 ± 0.7 Ma, (45.0 to 46.4 Ma), plus a Rb-Sr glauconitic mica isochron date on samples from immediately below the bentonite of 45.3 ± 0.3 Ma (45.0 to 45.6 Ma). These dates are analytically identical to the average of the K-Ar dates reported for the Warley Hill Formation. Ghosh (1972) reported two K-Ar dates from the lower Weches Formation in Texas which is also considered to correlate to calcareous nannofossil zone NP15. Although Ghosh (1972) did not indicate the analytical precision of the dates, we have assumed that their error is no more than 3 percent and discuss them using this error. The dates have also been recalculated using the IUGS K-Ar decay constants. Ghosh (1972) reported conventional K-Ar dates on glaucony from the lower Weches of 46.3 ± 1.4 Ma (44.9 to 47.4 Ma) from Burleson Bluff, Burleson County, and 46.7 ± 1.4 Ma (45.3 to 48.1 Ma) from just east of Nacogdoches, Nacogdoches County. These dates are in analytical agreement with the average of the K-Ar dates reported for the Warley Hill Formation, but also are older than the Rb-Sr isochron date (Figure 5). Siesser and Fitzgerald (1985) reported a Rb-Sr model date of primarily disordered to ordered glauconite from the Tallahatta Formation in Alabama of 42.7 ± 0.9 Ma. Although this agrees with the Rb-Sr isochron date reported here, it is younger than the other Rb-Sr and K-Ar dates reported from equivalent units in the southeastern and Atlantic Coastal Plain. Based upon this analysis, the Rb-Sr isochron date reported for the Warley Hill Formation is considered too young. The date could be too young as the result of post-diagenetic alteration of the Rb-Sr isotopic system. Evidence that such alteration may have occurred is provided by the initial $^{87}Sr/^{86}Sr$ ratio of 0.7084 ±

0.0012 which is higher than the Sr isotopic composition for middle Eocene seawater, and the high MSWD value of 5.3.

Upper Middle Eocene

The Chapel Branch Member of the Santee Limestone contains *Cubitostrea sellaeformis* which allows the unit to be correlated to the upper Lisbon Formation of Alabama, and sequence 2 of the Castle Hayne Limestone of North Carolina. The upper Lisbon Formation is assigned to calcareous nannofossil zones NP16-17 (Siesser, 1983; Mancini and Tew, 1988) as is sequence 2 of the Castle Hayne Limestone (Zullo and Harris, 1987). Calcareous nannofossil zones NP16-17 span intervals of time between 47.5 Ma and 37 Ma as indicated by the recent time scales illustrated in Figure 5. The Rb-Sr isochron date of 40.4 ± 0.8 Ma is analytically identical to the limits placed on zones NP16-17 by Hardenbol and Berggren (1978), Curry and Odin (1982), Berggren and others (1985), and Haq and others (1987), but is younger than the limits placed on the zones by Harland and others (1982). The isochron date also is older than the Rb-Sr isochron date 36.7 ± 0.6 Ma reported by Harris and others (1984) for *Cubitostrea sellaeformis*-bearing beds of the Santee Limestone in Berkeley County. In addition, this latter date is also younger than the numerical limits that are placed on zones NP16-17 of all time scales illustrated in Figure 5 except the Curry and Odin (1982) scale. If these dates are compared to the bentonite dates reported by Ghosh (1972) for the *Cubitostrea sellaeformis*-bearing Cook Mountain Formation of east Texas, and substantiated by Obradovich (1988), the 40.4 ± 0.8 (39.6 to 41.2 Ma) isochron date analytically agrees with the average date reported by Ghosh (1972) of 42.2 ± 1.3 Ma (40.9 to 43.5 Ma) and is close to the new date of 42.0 ± 0.4 Ma (41.6 to 42.4 Ma) reported by Obradovich (1988). In addition, Harris and others (1990) reported an average of two conventional K-Ar dates on glauconitic mica of 39.7 ± 1.6 Ma from beds that contain *Cubitostrea sellaeformis* in a core from Allendale County, South Carolina. Because the isochron date for the Chapel Branch Member of the Santee Limestone agrees well with both the K-Ar and Rb-Sr dates on correlative units, we suggest that the Chapel Branch date is geologically significant.

Upper Oligocene

The Ashley Formation is considered late Oligocene in age and was assigned by Hazel and others (1977) to nannofossil zone NP24. This zone is within the time interval from about 30.5 Ma to 25 Ma (Figure 5). The Rb-Sr isochron date of 26.2 ± 1.2 Ma (25.0 - 27.4 Ma) for the Ashley Formation is in agreement with the numerical limits placed on zone NP24 by Hardenbol and Berggren (1978), Curry and Odin (1982), and Harland and others (1982), but is younger than the limits placed on the zone by Berggren and others (1985) and Haq and others (1987) as shown in Figure 5. To our knowledge there are no other dates from the southeastern Atlantic and Gulf Coastal Plain reported for calcareous nannofossil zone NP24.

SUMMARY AND CONCLUSIONS

New Rb-Sr and K-Ar dates for middle Eocene and upper Oligocene sediments reported in this study are in general agreement with previously reported glauconite and bentonite dates of correlative units from North Carolina, Mississippi and Texas. However, the dates do not agree with any one currently recognized Paleogene time scale. Specific points to note are:

1. Glauconitic mica dates for Eocene and Oligocene sediments in Calhoun, Orangeburg, and Dorchester Counties, South Carolina are inconsistent but agree within their assigned errors with some previously reported volcanic mineral and glauconite dates from the southeastern Atlantic and Gulf Coastal Plains, and some recent time scales.

2. The stratotype of the Warley Hill Formation, which is assigned to calcareous nannofossil zone NP15, yields a Rb-Sr isochron date of 41.6 ± 1.5 Ma and an average conventional K-Ar date of 45.1 ± 1.7 Ma. The isochron date agrees with the numerical limits placed on zone NP15 by Curry and Odin (1982), but not with the limits placed on the zone by Hardenbol and Berggren (1978), Harland and others (1982), Berggren and others (1985), and Haq and others (1987). The average K-Ar date agrees with the limits placed on the zone by Hardenbol and Berggren (1978), Harland and others (1982), Berggren and others (1985), and Haq and others (1987), but not the limits placed on the zone by Curry and Odin (1982). The Rb-Sr isochron date for the Warley Hill Formation is considered to be younger than the time of deposition of the unit. The average K-Ar date is considered to approximate the time of sediment deposition.

3. Glauconitic micas from the Chapel Branch Member of the Santee Limestone, which is assigned to calcareous nannofossil zones NP16-17, yield a Rb-Sr isochron date of 40.4 ± 0.8 Ma. This date agrees with the numerical limits placed on nannofossil zones NP16-17 by Hardenbol and Berggren (1978), Curry and Odin (1982), Berggren and others (1985), and Haq and others (1987), but not the limits placed on the zones by Harland and others (1982). The isochron date also falls within the analytical uncertainties of reported conventional K-Ar dates of equivalent sediments in Allendale County, South Carolina, and Burleson County, Texas. It is analytically older than a date reported by Harris and others (1984) for equivalent beds of the Santee Limestone in Berkeley County, South Carolina. The Rb-Sr isochron date for the Chapel Branch Member of the Santee Limestone is considered to be geologically significant. The Rb-Sr isochron date of 36.7 ± 0.6 Ma for the Santee Limestone previously reported by Harris and others (1984) is now considered to be younger than the time of suggested sedimentation of the unit.

4. Glauconitic micas from the late Oligocene Ashley Formation of the Cooper Group, which is assigned to calcareous nannofossil zone NP24, yield a Rb-Sr isochron date of 26.2 ± 1.2 Ma. This date agrees with the numerical limits placed on calcareous nannofossil zone NP24 by Hardenbol and Berggren (1978), Curry and Odin (1982), and Harland and others (1982), but is younger than the limits placed on the zone by Berggren and others (1985) and Haq and others (1987). However, the date is considered to be geologically significant and

approximates the time of deposition.

5. Isotopic dates of glauconitic mica are too often viewed as absolute values with little consideration given to their analytical precision. In addition, glauconitic mica dates are often only compared to one time scale, and not to others that are commonly used. When all time scales are considered it becomes readily apparent that there are significant differences of opinion with respect to the time of occurrence of stage boundaries and standard fossil zones.

6. Few complementary dates on minerals that crystallize at high-temperature (e.g., biotite) are available from units that provide samples for glauconitic mica dates. Thus, it usually is impossible to make direct comparisons of dates from both realms. Therefore, as Obradovich (1988) has suggested, some other unifying method must be used to properly evaluate glauconitic mica dates.

ACKNOWLEDGMENTS

We thank DuPont de Nemours, operators of the Savannah River Plant until March of 1989, and in particular Van Price for providing financial support for this research. In addition, Gerald R. Baum of ARCO Oil and Gas Company, Anchorage, Alaska, is acknowledged for providing financial support for the K-Ar dates. We also thank Margaret Williamson for purifying the glauconitic mica concentrates that were dated by the K-Ar conventional method. The Program for Marine Sciences Research at the University of North Carolina at Wilmington provided released time from teaching and partial financial assistance to the first author. We also thank Victor A. Zullo, Robert E. Weems, and Roy Odom for providing suggestions for improvement of this manuscript.

APPENDIX 1. ANALYTICAL PROCEDURES AND LABORATORY METHODS

Glaucony-rich samples collected from three localities in the Santee River area of South Carolina were gently hand-crushed and screened into different sand-size fractions, washed in demineralized water, and air-dried with reagent-grade acetone. On the basis of magnetic susceptibility, glaucony was separated from each sample on a Frantz magnetic separator using optimum down-slope, side-slope, and intensity settings. These settings varied for each sample. Each separated fraction was washed in 0.1N HCl twice for 2 minutes each, acetone-dried and hand-picked of impurities. Based on microscopic examination each size fraction consisted of greater than 99 percent mammillated to lobate, or replaced fossil fragment glaucony.

Odin (1982) correlated the percentage of K_2O in glaucony with the measured distance between the 001 and 020 X-ray peaks. Using X-ray diffractometry traces of samples with known K_2O concentrations, Odin and Matter (1981) showed that the distance between the peaks expands as the concentration of K_2O decreases and shrinks as K_2O increases. Following this technique, all glaucony samples dated in this study consist of greater than 6 percent K_2O, and therefore, are evolved to highly-evolved glauconitic mica.

Sixteen glauconitic mica concentrations (greater than 99 percent purity) were

analyzed for Rb and Sr concentration, plus Sr isotopic composition by standard mass spectrometric techniques in the geochronology laboratory in the Department of Geology at the University of North Carolina at Chapel Hill. All $^{87}Sr/^{86}Sr$ values are reported relative to the Eimer and Amend Sr standard value of 0.70800 in order to maintain inter-laboratory standardization. Thirteen recent analyses of this standard in our laboratory give an average $^{87}Sr/^{86}Sr$ ratio of 0.70803 ± 0.00005 (one standard deviation). NBS K-feldspar standards 70a and 607, which are suggested as Rb-Sr age standards, have been repeatedly analyzed. Twenty-one analyses in our laboratory give an average age of 1377 ± 6 Ma (one standard deviation) using $\lambda 1.42 \times 10^{-11}$ yr^{-1} as the ^{87}Rb decay constant, and assuming an initial $^{87}Sr/^{86}Sr$ ratio of 0.710. All $^{87}Rb/^{86}Sr$ ratios were determined by isotope dilution. Based on recent work in our laboratory, one standard deviation analytical uncertainties are no more than 0.5 percent for $^{87}Rb/^{86}Sr$ and 0.025 percent for $^{87}Sr/^{86}Sr$ ratios. Isochron dates were determined using the technique of York (1969) and are reported along with the initial $^{87}Sr/^{86}Sr$ ratios and mean square of weighted deviates (MSWD) in Figures 2, 3, and 4. In addition, Rb-Sr model dates for all glauconitic micas are also reported in Table 1.

Two hand-picked splits of glauconitic mica were dated by the conventional K-Ar technique by Krueger Enterprises, Cambridge, Massachusetts. Decay constants used were $\beta = 4.962 \times 10^{-10} yr^{-1}$ and $(\lambda_\varepsilon + \lambda_\varepsilon) = 0.581 \times 10^{-10}$ yr^{-1} .

REFERENCES CITED

Baum, G. R., Collins, J. S., Jones, R. M., Madlinger, B. A., and Powell, R. J., 1980, Correlation of the Eocene strata of the Carolinas: South Carolina Geology, v. 24, p. 19-27.

Berggren, W. A., Kent, D. V., Flynn, J. J., and Van Couvering, J. V., 1985, Cenozoic geochronology: Geological Society of America Bulletin, v. 96, p. 1407-1418.

Cooke, C. W., and MacNeil, F. S., 1952, Tertiary stratigraphy of South Carolina: U. S. Geological Survey Professional Paper 243-B, 29 p.

Curry, D., and Odin, G. S., 1982, Dating the Palaeogene, *in* Odin, G. S., ed., Numerical dating in stratigraphy, Part I: Chichester, John Wiley and Sons, p. 607-630.

Dockery, D. T., III, 1980, The invertebrate macropaleontology of the Clarke County, Mississippi, area: Mississippi Department of Natural Resources, Bureau of Geology, Bulletin 122, 387 p.

Faure, G., 1988, Principles of isotope geology, 2nd ed., New York, John Wiley and Sons, 589p.

Ghosh, P. K., 1972, Use of bentonites and glauconites in potassium ^{40}/argon^{40} dating in Gulf Coast stratigraphy [Ph.D. dissert.]: Houston, Texas, Rice University, 136 p.

Hardenbol, J., and Berggren, W. A., 1978, A new Paleogene numerical time scale: American Association of Petroleum Geologists, Studies in Geology, v. 6, p. 213-234.

Haq, B. U., Hardenbol, J., and Vail, P. R., 1987, Chronology of fluctuating sea levels since the Triassic: Science, v. 235, p. 1136-1167.

Haq, B. U., Hardenbol, J., and Vail, P. R., 1988, Mesozoic and Cenozoic chronostratigraphy and cycles of sea-level change, *in* Wilgus, C. K. and others, eds., Sea-level changes: an integrated approach: Society of Economic Paleontologists and Mineralogists, Special Publication 42, p. 71-108.

Harland, W. B., Cox, A. V., Llewellyn, P. G., Pickton, C. A. G., Smith, D. G., and Walters, R., 1982, A geologic time scale: Cambridge, Cambridge University Press, 131 p.

Harris, W. B., 1982, Rubidium-strontium glaucony ages, southeastern Atlantic Coastal Plain, USA, *in* Odin, G. S., ed., Numerical dating in stratigraphy, Part I: Chichester, John Wiley and Sons, p. 593-606.

Harris, W. B., and Bottino, M. L., 1974, Rb-Sr study of Cretaceous lobate glauconite pellets, North Carolina: Geological Society of America Bulletin, v. 85, p. 1475-1478.

Harris, W. B., and Fullagar, P. D., 1982, Rb-Sr glauconite isochron, Twiggs Clay Member of Dry Branch Formation, Houston County, Georgia, *in* Nystrom, P. G., Jr., and Willoughby, R. H., eds., Geological investigations related to the stratigraphy in the kaolin mining district, Aiken County, South Carolina: Carolina Geological Society Field Trip Guidebook, p. 47-55.

Harris, W. B., Fullagar, P. D., and Winter, J., 1984, Rb-Sr glauconite ages, Sabinian, Claibornian and Jacksonian units, southeastern Atlantic Coastal Plain, U.S.A.: Palaeogeography, Palaeoclimatology, Palaeoecology, v. 47, p. 53-76.

Harris, W. B., and Fullagar, P. D., 1987, Rb-Sr radiometric ages of glauconite from Eocene carbonate, Berkeley County, South Carolina: South Carolina Geology, v. 31, p. 51-57.

Harris, W. B., and Fullagar, P. D., 1989, Comparison of Rb-Sr and K-Ar dates of middle Eocene bentonite and glauconite, southeastern Atlantic Coastal Plain: Geological Society of America Bulletin, v. 101, p. 573-577.

Harris, W. B., and Zullo, V. A., in press, Eocene and Oligocene stratigraphy of the Coastal Plain, *in* Horton, Jr., J. W., and Zullo, V. A., eds., The Geology of the Carolinas: Knoxville, University of Tennessee Press.

Harris, W. B., Zullo, V. A., Laws, R. A., and Harris, M. K., 1990, Paleogene sequence stratigraphy and chronostratigraphy of a core from Allendale County, South Carolina: Geological Society of America, Abstracts with Programs, v. 22, p. 17-18.

Hazel, J. E., Bybell, L. M., Christopher, R. A., Frederiksen, N. O., May, F. E., McLean, D. M., Poore, R. Z., Smith, C. C., Sohl, N. F., Valentine, P. C., and Witmer, R. J., 1977, Biostratigraphy of the deep corehole (Clubhouse Crossroads corehole 1) near Charleston, South Carolina, *in* Rankin, D. W., ed., Studies related to the Charleston, South Carolina earthquake of 1886; a preliminary report: U. S. Geological Survey Professional Paper 1028-F, p. 71-89.

Koepnick, R. B., Burke, W. H., Denison, R. E., Hetherington, E. A., Nelson, H. F., Otto, J. B., and Waite, L. E., 1985, Construction of the seawater $^{87}Sr/^{86}Sr$ curve for the Cenozoic and Cretaceous: supporting data: Chemical Geology, Isotope Geoscience Section, v. 58, p. 55-81.

Mancini, E. A., and Tew, B. H., 1988, Paleogene stratigraphy and

biostratigraphy of southern Alabama: Field Trip Guidebook, Gulf Coast Association of Geological Societies Annual Meeting, New Orleans, Louisiana, 63 p.

Nystrom, P. G., Jr., 1987, The Tertiary stratigraphy of the St Matthews 15-minute quadrangle, south-central South Carolina (abs.): Geological Society of America, Abstracts with Programs, v. 19, no. 2, p. 121.

Nystrom, P. G., Jr., Willoughby, R. H., and Price, L. K., 1988, The Cretaceous and Tertiary stratigraphy of the Upper Coastal Plain of South Carolina, *in* Upper Cretaceous and Cenozoic geology of the Southeastern Atlantic Coastal Plain, Field Trip Guidebook T172, South Carolina Geological Survey, p. 23-42.

Obradovich, J. D., 1964, Problems in the use of glauconite and related minerals in radioactivity dating [Ph.D. dissert.]: Berkeley, California, University of California, 93 p.

Obradovich, J. D., 1988, A different perspective on glauconite as a chronometer for geologic time scale studies: Paleoceanography, v. 3, p. 757-770.

Odin, G. S., 1982, Numerical dating in stratigraphy: New York, John Wiley and Sons, 2 vs., 1040 p.

Odin, G. S., and Matter, A., 1981, De glauconiarum origine: Sedimentology, v. 28, p. 611-641.

Odin, G. S., and Curry, D., 1985, The Palaeogene time-scale: radiometric dating versus magnetostratigraphic approach: Journal of the Geological Society of London, v. 142, p. 179-188.

Odin, G. S., and Fullagar, P. D., 1988, Geological significance of the glaucony facies, *in* Odin, G. S., ed., Green marine clays: Developments in Sedimentology, v. 45, New York, Elsevier Publishers, p. 295-332.

Powell, R. J., 1984, Lithostratigraphy, depositional environment, and sequence framework of the middle Eocene Santee Limestone, South Carolina Coastal Plain: Southeastern Geology, v. 25, p. 79-100.

Powell, R. J., and Baum, G. R., 1982, Eocene biostratigraphy of South Carolina and its relationship to Gulf Coastal Plain zonations and global changes of coastal onlap: Geological Society of America Bulletin, v. 93, p. 1099-1108.

Prothero, D. R., Denham, C. R., and Farmer, H. G., 1982, Oligocene calibration of the magnetic polarity time scale: Geology, v. 10, p. 650-653.

Siesser, W. G., 1983, Paleogene calcareous nannoplankton biostratigraphy: Mississippi, Alabama, and Tennessee: Mississippi Department of Natural Resources, Bureau of Geology Bulletin 125, 61 p.

Siesser, W. G. and Fitzgerald, B. G., 1985, Rb-Sr ages of Paleogene provincial stages, eastern Gulf Coastal Province: Southeastern Geology, v. 25, p. 199-206.

Stenzel, H. B., 1949, Successional speciation in paleontology: the case of the oysters of the sellaeformis stock: Evolution, v. p. 34-50.

Toulmin, L. D., 1977, Stratigraphic distribution of Paleocene and Eocene fossils in the eastern Gulf Coast region: Geologic Survey of Alabama Monograph 13, v. 1, 602 p.

Ward, L. W., Blackwelder, B. W., Gohn, G. S., and Poore, R. Z., 1979, Stratigraphic revision of Eocene, Oligocene, and Lower Miocene formations

of South Carolina: South Carolina Geologic Notes, v. 23, p. 2-43.
Weems, R. E., and Lemon, E. M., Jr., 1984a, Geologic map of the Mount Holly quadrangle, Berkeley and Charleston Counties, S. C.: U. S. Geological Survey Quadrangle Map GQ-1579.
Weems, R. E., and Lemon, E. M., Jr., 1984b, Geologic map of the Stallsville quadrangle, Dorchester and Charleston Counties, S. C.: U. S. Geological Survey Quadrangle Map GQ-1581.
Weems, R. E., and Lemon, E. M., Jr., 1988, Geologic map of the Ladson quadrangle, Berkeley, Charleston, and Dorchester Counties, S. C.: U. S. Geological Survey Quadrangle Map GQ-1630.
Weems, R. E., and Lemon, E. M., Jr., 1989, Geology of the Bethera, Cordesville, Huger and Kittredge Quadrangles, Berkeley County, S. C.: U. S. Geological Survey Miscellaneous Investigations Series, Map I-1854.
York, D., 1969, Least-squares fitting of a straight line with correlated errors: Earth and Planetary Science Letters, v. 5, p. 320-324.
Zullo, V. A. and Harris, W. B., 1987, Sequence stratigraphy, biostratigraphy, and correlation of Eocene through lower Miocene strata in North Carolina, *in* Ross, C. A., and Haman, D., eds., Timing and depositional history of eustatic sequences: Constraints on seismic stratigraphy: Cushman Foundation for Foraminiferal Research, Special Publication 24, p. 197-214.

DISCOVERY OF KOLBECKITE IN GEORGIA - TWO POSSIBLE LATTICES SUGGESTED

HAROLD L. WEBB[1]
OTTO C. KOPP[2]

Department of Geological Sciences
University of Tennessee
Knoxville, TN 37996-1410

O. BURL CAVIN
TOMMY J. HENSON

Metals and Ceramics Division
Oak Ridge National Laboratory[3]
Oak Ridge, TN 37831-6064

ABSTRACT

Several millimeter- to submillimeter-sized crystals of the rare mineral kolbeckite ($ScPO_4 \cdot 2H_2O$) were discovered on the exposed surface of a lignitic log in a kaolin mine in east-central Georgia. Associated minerals include pyrite, szomolnokite, rozenite and clay minerals. This is only the third reported occurrence of kolbeckite in the USA.

The X-ray diffraction pattern contains 48 identified peaks (far more than previous patterns), which can be indexed using either a monoclinic or an orthorhombic cell; however, the monoclinic cell gives a slightly better fit. The monoclinic cell (space group $P2_1/c$) has the following dimensions: $\underline{a} = 5.451 \pm 0.001$, $\underline{b} = 10.246 \pm 0.005$, $\underline{c} = 8.937 \pm 0.004$, $\beta = 90.50°$.

INTRODUCTION

Considerable confusion has surrounded the nomenclature of kolbeckite. Schrauf (1879) (cited in Hey and others, 1982) described a mineral, eggonite, as a cadmium silicate, but later retracted this information suggesting that the specimens were fakes. The observations of Krenner (1929) (cited in Hey and others, 1982) lent credibility to the existence of eggonite.

Edelmann (1926) first described the mineral kolbeckite, which was found on drusy quartz and chlorite gangue from the Sadisdorf copper mine near Schmiedeberg, Saxony. It was thought to be a beryllium silicophosphate. Larsen and Montgomery (1940) first described sterrettite from cavities in pseudowavellite (crandallite) from the variscite deposit in Fairfield, Utah. It had the same general chemical formula type as that of eggonite.

Bannister (1941) compared X-ray, optical and chemical data for these

---

[1] Present address, ECC America Inc., P.O. Box 471, Sandersville, GA 31082
[2] Adjunct Research and Development Participant, Metals and Ceramics Division, Oak Ridge National Laboratory, Oak Ridge, TN 37831
[3] Operated by Martin Marietta Energy Systems, Inc., under contract DE-AC05-840R21400 with the U.S. Department of Energy.

minerals. He concluded that eggonite and sterrettite were identical and suggested that the name eggonite be dropped. Mrose and Wappner (1959) studied sterrettite from Fairfield, Utah, eggonite from Felsobanya, Romania and kolbeckite from Schmiedeberg, Saxony, using X-ray diffraction. They confirmed that eggonite and sterrettite were identical. Sterrettite and kolbeckite were found to be isostructural and their unit cells identical to that of synthetic $ScPO_4 \cdot 2H_2O$, suggesting that the major cation was Sc rather than Al. Suggested formulas were $ScPO_4 \cdot 2H_2O$ for sterrettite and $(Sc,Be,Ca)(SiO_4,PO_4) \cdot 2H_2O$ for kolbeckite. Mrose (1965) found that kolbeckite from Saxony is really $ScPO_4.2H_2O$. XRF analyses confirmed the presence of scandium, making sterrettite and kolbeckite the first known scandium-bearing phosphates.

Fleischer (1966) discredited the names eggonite and sterrettite in favor of kolbeckite ($ScPO_4 \cdot 2H_2O$). More recently, Hey and others (1982), discussed the history of eggonite, kolbeckite, and sterrettite in detail. Although eggonite had 47 years priority, the IMA Commission on New Minerals and Mineral Names discredited eggonite and sterrettite (Nickel and Mandarino, 1987); hence, kolbeckite is now the approved name for this rare mineral.

A NEW OCCURRENCE OF KOLBECKITE

Several millimeter- to submillimeter-sized, pale blue-gray crystals were discovered on the surface of a well-preserved piece of lignified wood in a lens of carbonaceous clay with abundant pyrite. The lens was exposed in the highwall of a kaolin mine (Georgia Kaolin Co., Inc.) located about 80 km northeast of Macon, Georgia, and approximately 3 km east of Deepstep, Georgia, in the east-central Georgia kaolin clay district.

The stratigraphy of the area consists of Paleozoic igneous and metamorphic rocks which are unconformably overlain by a wedging sheet of Tertiary and Cretaceous sediments. The sedimentary rocks pinch out at the Fall Line (the boundary between the Piedmont and inner Atlantic and Gulf Coastal Plain physiographic provinces) and thicken seaward at a rate of 3 to 9 m/km (Pickering and Hurst, 1989). Commercial kaolin lenses occur at the top of the Tertiary Huber formation and are separated from overlying Upper Eocene sediments by a sharply defined unconformity. The age of the Huber Formation can best be described as Paleocene-Eocene. Clay lenses at the top of the Cretaceous sediments are separated from overlying sediments by a sharply defined unconformity and are overlain by beds of quartz sand, kaolinitic sand, and kaolin ranging from 5 to 10 m thick, which comprise the lower Huber Formation. Due to the paucity of fossils no specific age data has been determined at the locality from which the crystals were collected. Based on stratigraphic relationships and the physical properties of the enclosing kaolin, the lignified wood from which the samples were taken is thought to belong to the Late Cretaceous Buffalo Creek Formation (Pickering and Hurst, 1989).

IDENTIFICATION

The crystals found on the lignitic log appear to be orthorhombic and are

similar in morphology to simple tabular barite or celestite crystals (basal pinacoid and prism forms). See Figure 1. The crystals have a pale blue-gray color. An initial X-ray diffraction (XRD) analysis performed on a very small sample was inconclusive, in part because the presence of such a rare mineral was totally unexpected. A qualitative electron microprobe analysis of a crystal revealed major concentrations of scandium and phosphorus. Subsequent XRD analysis

Figure 1. Kolbeckite crystal on exposed surface of lignitic log. The long axis of the crystal is approximately 1 mm.

data (Table 1) confirmed the presence of kolbeckite. Other minerals found on the surface of the log were identified as pyrite, szomolnokite, rozenite, kaolinite and illite. Several weak diffraction lines in the kolbeckite pattern could not be identified.

The X-ray diffraction identification was performed with a Scintag, Inc. automated θ-2θ powder diffractometer equipped with a solid state detector and copper target X-ray source operating at 45 kv and 40 ma. A sample was prepared by crushing some of the crystals to a small particle size and mounting them onto an Si crystal, zero-background sample holder. The data were collected in a continuous scan from 5 to 105 degrees 2θ at a rate of 0.1 degrees 2θ per minute and digitized every 0.01 degree so as to yield highly accurate peak positions. The digitized data were analyzed using background subtraction and $K\alpha_2$ elimination, thus leaving peaks attributable only to $K\alpha_1$ diffraction (λ = 1.540598). Peak positions were determined more accurately by profile fitting of the net intensity data. No internal standard was used, but previous results on a high-purity quartz

sample gave good agreement of lattice parameters with published values (± 0.0002). We do not believe there was much preferred orientation in the X-ray powder sample; however, there was not sufficient material to remount and make subsequent runs to check for this.

Electron microprobe analyses of the exposed surface of a small crystal using a JEOL JSM-733 electron microprobe showed scandium and phosphorus to be the only heavy (atomic number >11) elements present in major quantities, although small amounts of aluminum and iron were detected. Ideal kolbeckite should contain 25.55 wt.% scandium and 17.60 wt.% phosphorus. A semi-quantitative microprobe analysis of a flat crystal face mounted approximately perpendicular to the electron beam was attempted. Elemental concentrations were calculated by comparing raw intensity data with that obtained from mounted and polished scandium and InP standards, using ZAF computerized correction curves (Scott and Love, 1983). Electron microprobe results ranged from 16.0 to 17.0 wt.% scandium, and 10.1 to 10.7 wt.% phosphorus. These calculated surface concentrations are lower than stoichiometric values; however, the scandium-to-phosphorus ratio (which ranged from 1.56 to 1.59) is reasonable when compared with the ideal Sc/P ratio of 1.45. The difference between the measured surface composition and ideal composition could be the result of inclusions of organic material, crystal surface degradation due to localized heating by the electron beam, correction uncertainties, surface topography, or a combination of these factors.

There are only two previously reported occurrences of kolbeckite in the United States. One is in massive pseudowavellite (crandallite) in the variscite deposit of Fairfield, Utah (Larsen and Montgomery, 1940). The other is at the Union Carbide Vanadium Mine in Potash Sulfur Springs, Garland County, Arkansas (Hey and others, 1982), where the kolbeckite occurs in vugs on diopside-hedenbergite in the vanadium ore.

The presence of these kolbeckite crystals on the surface of a lignitic log is quite unusual. Given the small size and euhedral nature of the crystals on the exposed surface (typical of open-space filling), it is possible that these crystals formed after the mine was opened, but we have no specific information concerning the conditions under which they were deposited. Scandium occurs in trace amounts in many geologic materials, including coal, and is generally considered to be derived from igneous sources. Qualitative XRF analyses of lignitic samples away from the surface on which the crystals were found detected the presence of both scandium and vanadium. Scandium was also detected in the gray, carbonaceous clay adjacent to the lignite.

The scandium required to form these kolbeckite crystals may have been made available through the weathering of Paleozoic igneous and metamorphic rocks in the Piedmont. The trivalent scandium released could have been adsorbed onto clay surfaces, transported, and subsequently deposited along with abundant organic material (a source for the phosphorus) in this former delta front to marginal marine environment. Upon opening of the mine, the exposed lignitic log could have served as a conduit for fluid from which the kolbeckite precipitated.

Table 1. X-ray Powder Diffraction Data for Georgia Kolbeckite

Georgia kolbeckite		Orthorhombic		Monoclinic	
I_{obs}	d_{obs}	d_{calc}	hkl	d_{calc}	hkl
3	6.753	6.737	011	6.735	011
16	5.130	5.128	020	5.123	020
100	4.819	4.809	110	4.813	110
4	4.673	4.650	101	4.672	-101
17	4.473	4.468	002	4.468	002
29	3.734	3.733	120	3.733	-120
2	3.436	3.445	121	3.437	121
6	2.895	2.895	130	2.894	-130
36	2.853	2.865	122	2.857	122
1	2.748	2.754	131	2.750	131
1	2.714	2.715	032	2.714	032
2	2.632	2.632	210	2.634	-210
4	2.522	2.524	211	2.521	-211
1	2.429	2.430	132	2.424	132
1	2.409	2.405	220	2.406	-220
2	2.338	2.328	123	2.336	-202
1	2.319	2.320	140	2.318	-140
1	2.245	2.245	141	2.245	033
1	2.234	2.234	004	2.234	004
1	2.183	2.183	014	2.183	014
2	2.050	2.048	024	2.048	024
1	1.997	1.999	051	1.997	051
1	1.921	1.919	150	1.922	-124
2	1.880	1.877	151	1.879	-223
1	1.860	1.867	240	1.863	052
<1	1.834	1.830	143	1.833	-143
1	1.761	1.764	152	1.761	152
2	1.713	1.711	320	1.713	-320
1	1.703	1.703	214	1.703	-105
2	1.636	1.638	250	1.638	-250
3	1.606	1.604	161	1.606	144
<1	1.574	1.578	331	1.577	331
<1	1.567	1.550	303	1.557	-303
1	1.541	1.542	234	1.541	-252
<1	1.533	1.533	313	1.532	-162
9	1.523	1.521	135	1.524	-135
<1	1.451	1.456	154	1.453	154
5	1.440	1.437	106	1.440	-225
<1	1.425	1.423	116	1.426	-116
<1	1.415	1.415	170	1.417	-333
1	1.349[1]	1.350[1]	410	1.349	-172
<1	1.327	1.326	343	1.327	-136
<1	1.314	1.316	420	1.314	073
1	1.304	1.302	334	1.305	-421
<1	1.288	1.288	046	1.288	046
2	1.275	1.274	305	1.276	271
<1	1.201	1.199	362	1.202	-182
8	1.1141	1.117	008	1.1166	147

[1]Note: the calculated orthorhombic pattern also contains peaks at 1.346 Å (401) and 1.347 Å (055); however, these peaks could be masked by the peak at 1.349 Å.

IS KOLBECKITE MONOCLINIC OR ORTHORHOMBIC?

The diffraction pattern for Georgia kolbeckite matches the diffraction patterns for kolbeckite from Utah (Mrose and Wappner, 1959) and Austria (Postl, 1981) quite well; however, our pattern contains many additional peaks not found in either of those patterns.

Hey and others (1982), report that eggonite (kolbeckite) from all localities is monoclinic, whereas Mrose and Wappner (1959) had indexed Utah kolbeckite on the basis of an orthorhombic cell. The large number of peaks (a total of 48 lines) recorded for our Georgia kolbeckite sample provided an opportunity to determine its lattice parameters more accurately.

The results are compared in Tables 1 and 2. The data were indexed on the basis of both an orthorhombic lattice (space group $P2_12_12_1$) and a monoclinic lattice (space group $P2_1/c$). In both cases, it was possible to index all the lines. The data had been obtained using an extremely slow scan rate (0.1 degree 2θ per minute), yielding peaks with good statistics even though the sample volume was small.

Table 2. Comparison of Cell Dimensions for Kolbeckite.

Sample	System	a	b	c	β
Georgia	Orthorhombic	5.445 ±0.003	10.255 ±0.007	8.936 ±0.005	
Georgia	Monoclinic	5.451 ±0.001	10.246 ±0.005	8.937 ±0.004	90.50
Utah[1]	Orthorhombic	5.44	10.22	8.92	
Austria[2]	Monoclinic	5.418	10.193	8.893	90.8[3]

[1] Mrose and Wappner (1959).
[2] Postl (1981).
[3] Note that the β angle given on JCPDS card 38-431 is 90.8°; however, a brief abstract in Chemical Abstracts (v. 96, 1982, 96:184384q) gives the β value as 90°48'.

Based on the analytical precisions obtained through least-squares refinement (Table 2), the monoclinic lattice provides a slightly better fit than does the orthorhombic lattice; however, all the peaks could be indexed using either the monoclinic or the orthorhombic lattice. From our observations and the limited number of diffraction maximum observed by Mrose and Wappner (1959), it is easy to see how their pattern was indexed on the less complicated orthorhombic lattice. Indeed, the monoclinic beta angle is very near 90° thus making the lattice appear

orthorhombic.

Perhaps the wisest course of action would be to postpone making any final judgement concerning the proper space group for kolbeckite until a thorough structural analysis can be performed. It is even possible that both monoclinic and orthorhombic polymorphs exist.

ACKNOWLEDGEMENTS

We wish to thank Georgia Kaolin Co., Inc., and Sam Pickering for access to the mine and for his thought-provoking discussions. We appreciate the helpful suggestions made by Roland Rouse, University of Michigan, and Camden R. Hubbard, Metals and Ceramics Division, Oak Ridge National Laboratory. The authors also wish to thank the reviewers, F. Donald Bloss (Virginia Polytechnic Institute and State University) and Daniel J. Milton (US Geological Survey) for their careful reviews and comments.

REFERENCES

Bannister, F.A., 1941, The identity of "eggonite" with sterrettite: Mineralogical Magazine, v. 26, p. 131-133.

Edelmann, F., 1926, Kolbeckite, a new mineral from Saxony: Jahrb. Berg-u-Hutten w. Sachsen. v. 100, p. 73-74 [not seen; extracted from American Mineralogist, v. 13, p. 592, 1928].

Fleischer, M., 1966, Index of new mineral names, discredited minerals and changes of mineralogical nomenclature in Volumes 1-50 of The American Mineralogist: American Mineralogist, v. 51, p. 1247-1357.

Hey, M.H., Milton, C. and Dwornik, E., 1982, Eggonite (kolbeckite, sterrettite), $ScPO_4 \cdot 2H_2O$: Mineralogical Magazine, v. 46, p. 493-497.

Larsen, E.S. and Montgomery, A., 1940, Sterrettite, a new mineral from Fairfield, Utah: American Mineralogist, v. 25, p. 513-518.

Mrose, M.E., 1965, New specific refractive energy values for CuO and Sc_2O_3: American Mineralogist, v. 50, p. 288.

Mrose, M.E. and Wappner, B., 1959, New data on the hydrated scandium phosphate minerals: sterrettite, "eggonite", and kolbeckite: Bulletin of the Geological Society of America, v. 70, p. 1648-1649.

Nickel, E.H. and Mandarino, J.A., 1987, Procedures involving the IMA Commission on New Minerals and New Mineral Names and guidelines on mineral nomenclature: American Mineralogist, v. 72, p. 1031-1042.

Pickering, S.M. and Hurst, V.J., 1989, Commercial Kaolins in Georgia, Occurrence, Mineralogy, Origin and Use, *in* W.J. Fritz, ed., Excursions in Georgia Geology, v. 9, p. 29-75. Georgia Geological Society, Atlanta, GA 30303.

Postl, W., 1981, Kolbeckit, ein seltenes wasserhaeltiges Scandiumphosphat aus dem Steinbruch in der Klause bei Gleichenberg, Steiermark: (Kolbeckite, a rare hydrated scandium phosphate from the Klause quarry near Gleichenberg, Styria): Mitteilungsblatt Abteilung fuer Mineralogie am Landesmuseum

Joanneum, v. 49, p. 23-29.
Scott, V.D. and Love, G., 1983, Quantitative Electron-Probe Microanalysis: John Wiley and Sons, Inc., New York, 345pp.

MIXING ZONE HYDROCHEMISTRY WITHIN A CONFINED AQUIFER SYSTEM: CUMBERLAND ISLAND, GEORGIA

STEPHEN K. WILSON
SETH ROSE
RAM ARORA
JENNIFER HERNDON

Department of Geology
Georgia State University
Atlanta, Georgia 30303

STEPHEN COFER-SHABICA

National Park Service
Institute of Ecology
University of Georgia
Athens, Georgia, 30602

ABSTRACT

The water chemistry of a multiple-aquifer system underlying Cumberland Island, Georgia was investigated in order to identify possible saltwater intrusion and to better understand the geochemical dynamics of freshwater/seawater mixing within this setting. Brackish water (3-88% seawater) was present within the thin and lithologically complex Pliocene-Miocene aquifer system. Carbon-14 dating of groundwater within this mixing zone indicated that the freshwater component was at least several thousand years old and that the saline component was recent seawater. Possible sources of seawater include a natural offshore exposure and a manmade navigational channel immediately south and west of the island.

Magnesium was the only ion which mixed conservatively within the Pliocene-Miocene aquifer. Bicarbonate and calcium ion concentrations deviated greatly from the freshwater-seawater mixing line. Inferred geochemical processes affecting the composition of groundwater within the Pliocene-Miocene aquifer include possible calcite dissolution, sulfate reduction (occurring in local anaerobic zones) and the exchange of calcium ion for sodium (reverse ion exchange). Sulfate reduction has probably resulted in the high bicarbonate alkalinity observed in several locations. Reverse ion exchange, as evidenced by sodium concentrations lower than those predicted from simple mixing, is probably a factor responsible for the calcium-chloride water type observed within the dilute portion of the mixing zone.

INTRODUCTION

The mixing of continentally derived groundwater with seawater (saltwater intrusion) is a problem that continues to be of interest to the sciences of hydrology (Reilly and Goodman, 1985), aqueous geochemistry (Stoessel and others, 1989 and Sanford and Konikow, 1989) and water-resources management. The stability of the carbonate minerals within mixing zones has been particularly controversial and has evoked great interest (Hanshaw and others, 1971 and Hardie, 1987). Other aspects of mixing zone systematics, such as the geochemistry of the alkali elements and

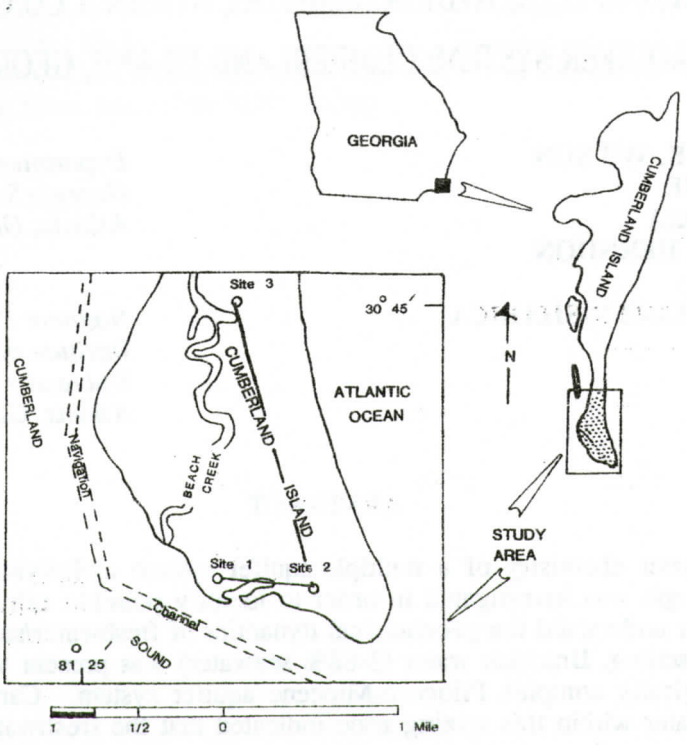

Figure 1. Map of the study area showing well-site locations on the southern portion of Cumberland Island. The lines connecting sites 1, 2 and 3 represent the hydrostratigraphic section shown on Figure 2.

sulfate, have received less attention and will be addressed in this present study.

The objective of this study was to analyze the effects of modern seawater intrusion within a complex multiple-aquifer system underlying the southern portion of Cumberland Island, the largest and southernmost barrier island along the coast of Georgia (Figure 1). Although barrier islands are prominent geomorphic features on the Atlantic and Gulf Coasts, there have been relatively few studies which have carefully documented the groundwater chemistry within their underlying aquifers.

Cumberland Island, a protected National Seashore within the U.S. National Park System, is approximately 16 miles long and 0.5 to 3 miles wide. Beginning in the early 1950's, Cumberland Island Sound, adjacent to the southern portion of the island was dredged for navigational purposes (Figure 1). In the 1960's the channel was deepened to 42 feet to accomodate the U.S. Navy's Poseidon submarines based at King's Bay, Georgia. The channel was again deepened in the late 1980's to a depth of 51 feet below mean sea level, thereby breaching an aquiclude and possibly exposing the confined Pliocene-Miocene aquifer to seawater. Numerous test wells were drilled through the channel bed prior to dredging during the 1980's and these may have also provided conduits for seawater contamination. Recently, questions have been raised about the possible effects of these manipulations upon groundwater quality; hence, this study was undertaken to gather the hydrochemical

data necessary to address these concerns.

METHODS

Three clusters of monitoring wells, constructed of four- inch diameter polyvinyl chloride (PVC), were completed within the Holocene-Pleistocene surficial aquifer and the underlying Pliocene-Miocene and Miocene confined aquifers (Figure 2). The deepest boring (Well 1) was sampled continuously to refusal with a split-spoon sampler and core samples were recovered thereafter. Further lithological details were interpreted from cuttings of the other wells. The deepest borehole at each site was geophysically logged with natural gamma, resistivity, and spontaneous potential logs to facilitate stratigraphic correlation. Water levels in each of the boreholes were measured with a multi-channel pressure transducer and assigned an absolute elevation after a topographic survey was conducted. To prepare a potentiometric surface map, water levels at each well-site were converted upon the basis of density (as determined by salinity) to the equivalent freshwater head.

Specific conductance, alkalinity, water temperature, and dissolved oxygen concentrations were monitored in the field. The well bores were purged by pumping prior to sampling. After temperature and conductivity stabilized, groundwater samples were retrieved in polyethylene bottles for chemical anlaysis. Samples used for the analysis of calcium, magnesium, sodium, and potassium were filtered through a 0.45 micron membrane and preserved at a pH of less than 2 with concentrated nitric acid. Cation concentrations were determined using atomic absorption spectrophotometry. Anion concentrations, including sulfide, were determined using standard potentiometric and colorimetric procedures detailed in Wilson (1990). All wells were resampled approximately six months later in order to assess seasonal variation. We primarily relied upon the results of the second sampling period in that the associated analytical error was smaller than the first period. Unfortunately, equipment failure during the second sampling period prevented the field measurement of pH at many of the well sites; therefore, laboratory values are reported. Thermodynamic speciation of the inorganic ions and saturation indices were calculated using WATEQF (Plummer and others, 1976).

Three 50-liter samples were taken from the Pliocene-Miocene aquifers for carbon-14 age analysis. Age-estimates of the groundwater within the mixing zone were made by the Center for Applied Isotope Studies at the University of Georgia based upon the carbon-14 activity of the $BaCO_3$ precipitated from the samples. The carbon-14 activity was determined by a benzene synthesis/liquid scintillation counting technique.

RESULTS

Hydrogeology

The most permeable units underlying Cumberland Island (Figure 2) consist of the surficial Holocene-Pleistocene aquifer (sands), the Pliocene-Miocene aquifer

(carbonate rock and sediment), the Miocene aquifer (calcareous sands) and the Floridan aquifer (carbonate rock). The Floridan aquifer was not monitored as part of this study. The surficial aquifer was approximately 45 feet thick and was comprised mostly of siliceous sand and calcareous shells.

The Pliocene-Miocene aquifer, the principal concern of this study, is overlain by a complex Pleistocene confining unit. The Pliocene-Miocene aquifer consists of carbonate sands (the age- equivalent of the Duplin Formation) and an underlying fossiliferous dolomite unit of the Miocene Charlton Formation (McLemore and others, 1981). The upper portion of the dolomite includes horizons of calcite and aragonite shells, as well as molds and casts. Zones of vugs, fractures, and cavities were also present within this unit. The Pliocene-Miocene aquifer is approximately 30 feet thick in the study area and is confined by overlying Pleistocene clay units (which alternate with sands) and an underlying argillaceous dolomite. The Pliocene-Miocene units are not areally extensive and therefore are difficult to correlate over appreciable distances. This was particularly evident when attempting to correlate lithological units from the shoreline sites 1 and 2 with the inland site 3 (a distance of approximately two miles).

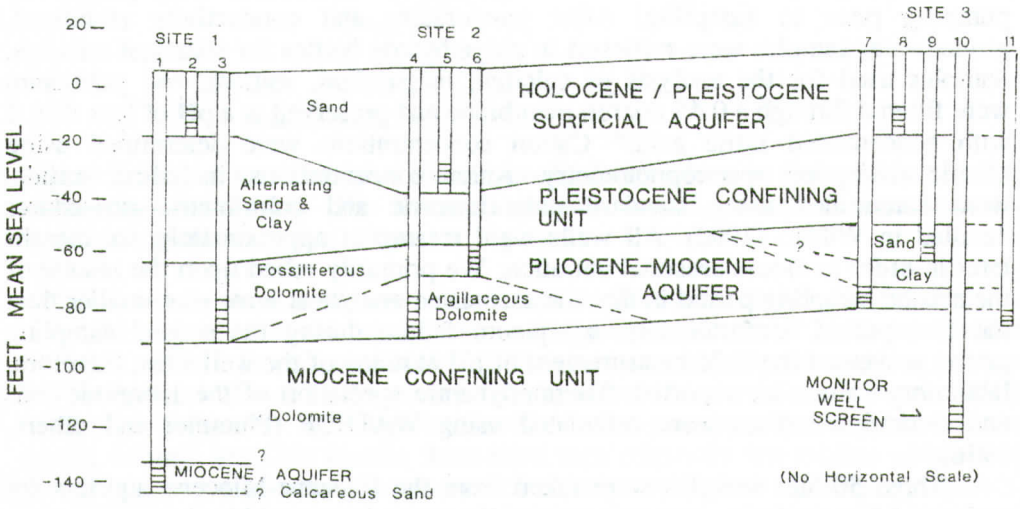

Figure 2. Hydrostratigraphic section showing location of the monitoring well screens and the various aquifers and confining units. The location of the well clusters are shown on Figure 1. Well #11 existed as a production well and was constructed prior to this investigation.

The Miocene aquifer, comprised predominantly of calcareous sands, is stratigraphically part of the Charlton Formation (McLemore and others, 1981). The upper portion of this aquifer was penetrated only by well 1 and therefore we cannot determine the areal extent of this aquifer below the study area. For purposes of discussion we typically include the Miocene aquifer with the overlying Pliocene-Miocene aquifer.

Water levels and salinities (Table 1) were distinct within virtually all wells at each site. This suggests that the confining beds are at least somewhat effective, the aquifers shown on Figure 2 are distinct, and the Pliocene-Miocene aquifer is in fact confined. The water level variations with respect to the different units also indicate that vertical leakage between these units is possible.

Table 1. Water Levels and Percentage Seawater

Well Number	Aquifer	Water Level[1] Feet msl.	Percentage Seawater
1	Miocene	1.80	32
2	Surficial	0.50	0
3	Pliocene-Miocene	1.67	68
4	Pliocene-Miocene	5.52	73
5	Surficial	4.44	3
6	Pliocene-Miocene	5.32	88
7	Pliocene-Miocene	2.62	4
8	Surficial	4.93	0
9	Pliocene-Miocene	2.48	0
10[2]	Pliocene-Miocene	2.58	0
11	Pliocene-Miocene	2.62	5

[1]Measurements made June 28, 1990; Water levels correspond to freshwater head, computed upon the basis of density
[2]Well 10 is completed within a confining unit

The principal recharge area for the Pliocene-Miocene aquifer is presumably located inland within the Coastal Plain of Georgia. However, the potentiometric surface (Figure 3) measured June 28, 1990, indicates that groundwater flow in the southern portion of the island is predominantly from east to west. This may be due to an offshore exposure which provides a local source of recharge. Unfortunately, we do not have sufficient data to describe the exact location and extent of this possible exposure. Work is ongoing to determine the effects of tidal fluctuations upon the direction(s) of groundwater flow within the study area.

Similar water levels in wells 4 and 6 at site 2 indicate a hydraulic connection between the upper zone of relatively high permeability (fossiliferous dolomite) and the lower argillaceous dolomite. Interestingly, groundwater was 15% more saline (i.e. more dense) in the overlying well 6 than in well 4 (Table 1 and Figure 2). This density inversion is likely the result of the heterogeneity encountered at well-site 2. Vacher (1978) has previously shown that saltwater intrudes further inland below oceanic islands in high-permeability zones. Apparently seawater is preferentially intruding the more permeable upper fossiliferous dolomite within the Pliocene-Miocene unit.

Unfortunately, the well-control was not sufficient to accurately map a zone of dispersion within the Pliocene-Miocene aquifer. We note the shoreline sites 1 and 2 were characterized by brackish water (chloride = 6,000 to 17,000 mg/l) while the highest chloride concentration at the inland site 3 was 600 mg/l. Therefore, the zone of dispersion may extend throughout the Pliocene-Miocene aquifer in the

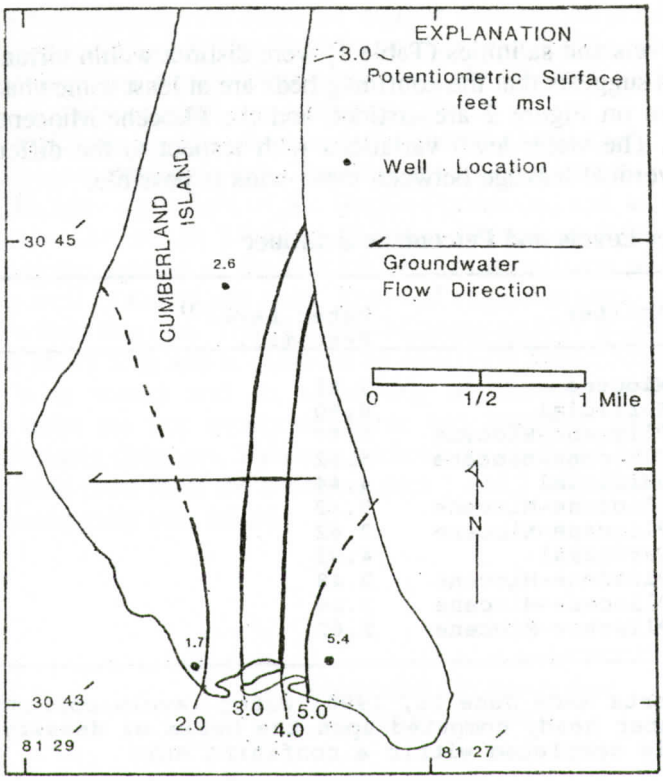

Figure 3. The potentiometric surface for the Pliocene-Miocene aquifer at high tide on June 28, 1990.

southern part of Cumberland Island.

Hydrochemistry

The groundwater chemistry of the surficial aquifer (as monitored by wells 2,5, and 8; Figure 2) is both spatially and temporally variable and is dominated by Ca-HCO_3 and Na-Cl water types. The chloride concentration for well 5 completed within the surficial aquifer at site 2 was 580 mg/l. However, the chloride concentration at site 1, located slightly closer to the ocean, was 40 mg/l. Therefore, the chloride concentration observed in well 5 cannot be readily attributed to seawater mixing. The mechanisms for the slight salinization of the surficial aquifer likely involve the concentration of sea spray within the vadose zone and/or local recharge of poor-quality water from the occasional flooding of salt-marshes. Groundwater was anaerobic at well 5, probably due to an influx of organic matter within salt-marsh recharge.

The Pliocene-Miocene aquifers were characterized by many different water types - sodium/chloride at well locations 1,3,4, and 6 (Figure 2); calcium/chloride (wells 7 and 11) and calcium/bicarbonate (wells 9 and 10). To illustrate the spatial

geochemical variability, we note that the alkalinity of groundwater derived from well 3 was approximately twice that of well 6; yet both of these wells were completed within a highly saline portion of the fossiliferous dolomite and were located only about 3,000 feet from one another.

Chloride concentrations, expressed as a fraction of seawater, varied from 0 (well 9) to 88% (well 6). Sodium-chloride ratios approached that of seawater (Na/Cl = 0.85; Berner and Berner, 1987) within the more saline groundwater but differed significantly from this ratio at lower salinities. Notably, the Na/Cl ratio for well 7 (salinity = 3% seawater) was 0.31. This indicates some process other than the simple dilution of seawater with freshwater. Likely these ionic ratios are indicative of ion exchange, as subsequently discussed.

DISCUSSION

Apparent Carbon-14 Ages and Other Implications

Carbon-14 measurement has been shown to be a useful tool in assessing the origin of salts within coastal zones. Hanshaw and others (1965) noted that increased activity of carbon-14 within the more saline water, relative to the fresher water, may indicate recent ocean water as the source of contamination. In turn, decreased carbon-14 activity within the saline water, relative to freshwater, may indicate residual (Pleistocene?) seawater which has not yet been flushed from a coastal aquifer.

The apparent carbon-14 ages for wells 4,3, and 7 completed within the Pliocene-Miocene aquifer decreased inversely and linearly as a function of chloride concentration or percentage seawater (Figure 4). This indicates that fresh groundwater, relatively distal from its recharge area, is mixing with recent seawater. The approximate 8,000-year age associated with the freshest water (3% seawater; well 7) is probably too old in that we have not corrected for the possible dissolution of the carbonate matrix. Nonetheless, we conclude from the large difference between apparent ages, that the brackish groundwater represents a mixture of relatively "mature" freshwater with recent seawater as indicated by Figure 4. This is important because saline water within other Atlantic Coastal Plain barrier islands (e.g. Hatteras Island, North Carolina) has been attributed to the entrapment of residual salts rather than the intrusion of modern seawater (Harris, 1967).

Mixing Trends

The first-order chemical dynamics of freshwater/saltwater mixing can often be inferred from simple mixing lines (Figures 5a-f) in that deviations with respect to these mixing-lines indicate some process or processes other than simple, two end-member physical mixing. Construction of the mixing lines was facilitated by the wide range of salinities observed within the Pliocene-Miocene groundwater. The percentage of seawater in these figures represents the measured chloride concentration of a given sample related to seawater (Cl = 545.95 mmol/l; Berner and Berner, 1987).

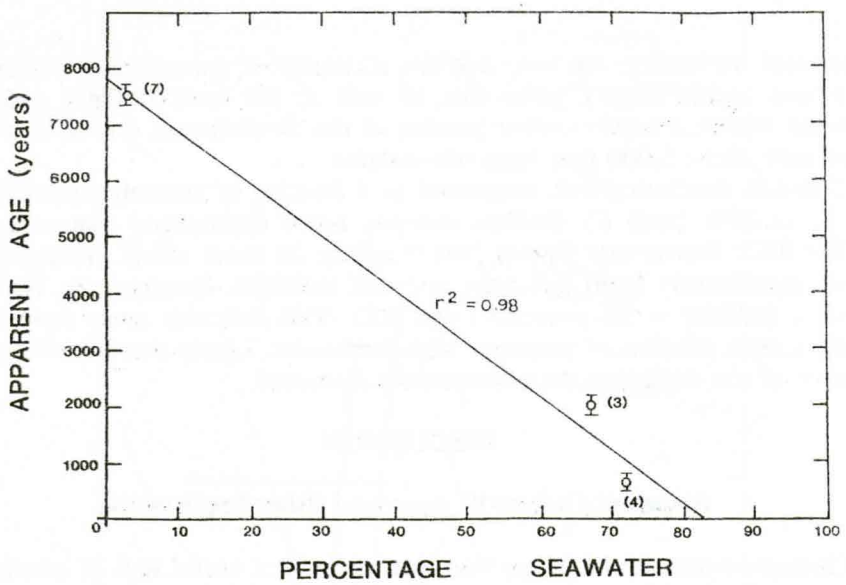

Figure 4. The relationship between apparent groundwater age within the Pliocene-Miocene aquifer system and percentage seawater. The error bars indicate analytical error and the number in parenthesis indicates the well number.

Magnesium was apparently the only major ion to mix conservatively over the wide range of salinities observed within the Pliocene-Miocene aquifer (Figure 5d). Sodium ion concentrations in the more dilute brackish water (seawater percentage < 10%) were less than those concentrations which would result from simple mixing (Figure 5a). Potassium and sulfate concentrations consistently plotted below the mixing line (Figures 5b and f). The most obvious deviations from simple mixing occurred with respect to the calcium and bicarbonate ion concentrations (Figures 5c and 5e). WATEQF-calculated PCO_2 values varied by an order of magnitude (Table 2). We therefore conclude the wide range of bicarbonate alkalinity concentrations observed within the Pliocene-Miocene aquifers is principally the result of the variable production of carbon dioxide within organic-rich zones. Other factors controlling alkalinity within this aquifer include possible calcite dissolution and sulfate reduction. These inferred local organic-rich zones or lenses can also be used to explain the sulfate and dissolved oxygen variability (Table 2), as subsequently discussed.

For purpose of comparison, the bicarbonate concentrations within the Pliocene-Miocene aquifer at Cumberland Island varied markedly from those observed in mixing zones within the coastal carbonate aquifer of the Yucatan Peninsula. Stoessel and others (1989) found a simple negative linear trend with respect to alkalinity and percentage seawater in the Yucatan mixing zones which indicated that seawater dilution was the dominant process affecting alkalinity. Here within the Pliocene-Miocene aquifer underlying Cumberland Island, the processes controlling alkalinity are far more complex.

The sulfate concentrations at Cumberland Island were consistently one to

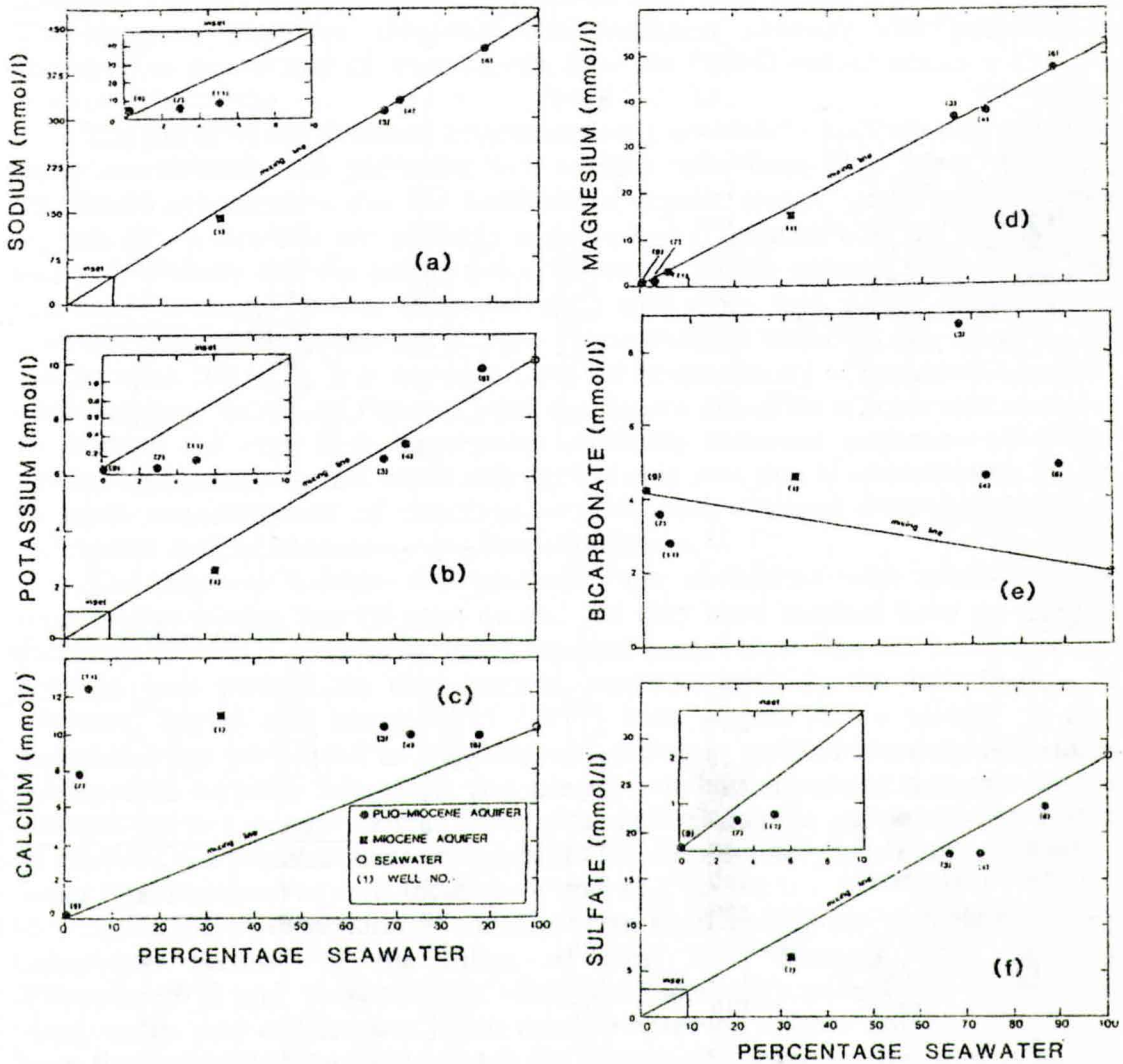

Figure 5. Major ion constinuency of groundwater related to the percentage of seawater within the Pliocene-Miocene aquifers. Deviations which occur with respect to each "mixing line" are discussed in the text. The mixing line represents the conservative mixing of seawater with fresh carbonate groundwater (well 9). The water chemistry for well 10 was not included in that this well was completed in an aquitard within the Pliocene-Miocene units.

two millimoles lower than those predicted to result from conservative mixing (Figure 5f). Groundwater throughout the mixing zone was approximately one to two orders of magnitude undersaturated with respect to gypsum; therefore, the sulfate ion concentrations cannot be readily attributed to gypsum precipitation. Furthermore, these concentrations cannot be explained by the mixing of seawater with a freshwater component other than that represented by well 9. This is the case because the freshwater component would have to be characterized by a "negative" sulfate concentration in order to draw a line through the data points.

The most likely reaction affecting sulfate concentrations involves the

Table 2. Chemical Analyses

WELL NO.[1]	1	2	3	4	5
lab pH	7.43	8.02	7.08	7.43	8.14
D.O. (mg/l)	0.0	4.5	0.0	4.7	0.0
Temperature (°C)	22.8	20.1	22.0	21.6	21.8
Calcium (mg/l)	440	85	420	400	24
Magnesium (mg/l)	380	19	920	940	52
Sodium (mg/l)	3,200	52	7,300	7,600	380
Potassium (mg/l)	92	5.5	260	280	28
Bicarbonate (mg/l)	283	403	523	285	319
Sulfate (mg/l)	650	18	1,700	1,700	62
Sulfide (mg/l)	7.7	0.2	56.2	4.0	70
Chloride (mg/l)	6,200	40	13,000	14,000	580
Silica (mg/l)	51	22	28	26	34
TDS (mg/l)	11,152	440	23,885	25,086	1,318
Percent Error[2]	0.43	0.49	1.22	0.00	-0.47
log PCO_2[3]	-2.15	-2.48	-1.54	-1.85	-2.71
Calcite S.I.[4]	0.53	0.97	0.25	0.00	0.36

WELL NO.[1]	6	7	8	9	10	11
lab pH	7.43	7.60	6.62	7.64	7.92	7.72
D.O. (mg/l)	2.0	2.7	3.3	4.0	2.0	1.8
Temperature (°C)	21.8	22.8	20.9	20.9	20.9	21.2
Calcium (mg/l)	400	320	51	76	75	500
Magnesium (mg/l)	1,200	17	10	2.8	10	28
Sodium (mg/l)	9,600	120	77	31	25	200
Potassium (mg/l)	380	3.3	4.9	1.6	2.1	4.9
Bicarbonate	297	217	77	256	255	169
Sulfate (mg/l)	2,200	60	71	2	41	95
Sulfide (mg/l)	0.3	0.2	0.1	0.3	0.5	0.5
Chloride (mg/l)	17,000	600	140	43	29	1,000
Silica (mg/l)	13	56	5.7	64	36	54
TDS (mg/l)	30,940	1,285	398	347	344	1,965
Percent Error[2]	1.46	2.16	1.09	-1.42	4.52	4.50
log PCO_2[3]	-2.21	-2.34	-1.77	-2.27	-2.56	-2.61
Calcite S.I.[4]	0.32	0.78	-0.45	0.41	0.66	0.89

[1] Analyses for December, 1989

[2] Percent Error = $\frac{\text{Sum of meq cations - Sum of meq anions}}{\text{Sum of meq cations + Sum of meq cations}}$

[3] Computed from WATEQF (Plummer and others, 1976)

[4] S.I. = Saturation Index = Log10 Ion Activity Product/Kt where Kt = equilibrium constant at a given temperature

anaerobic reduction of sulfate (Berner and Berner, 1987):

$$2CH_2O + SO_4^{-2} \longrightarrow H_2S + 2HCO_3^- \qquad [1]$$

All of the groundwater sampled showed the effects of sulfate reduction; however,

dissolved oxygen concentrations approached zero only at site 1 (wells 1 and 3). The apparent dissolved oxygen/sulfate reduction anomaly can possibly be attributed to the mixing of waters from different "micro-redox" zones within the zone of dispersion.

The presence of dissolved oxygen does not necessarily indicate that all of the water contributing to a particular well sample came from oxic zones. We have previously hypothesized that the oxidation of organic matter occurs locally within organic-rich lenses that are probably more or less coincident with the argillaceous zones. It is likely that the sulfate reduction occurs within some of these zones and this water ultimately mixes (convectively?) with more oxic water, producing the low, but measurable, dissolved oxygen concentrations observed elsewhere in the mixing zone (Table 2). It is apparent from the stoichiometry of Equation 1 and the concentrations shown on Figure 5f that the degree of sulfate reduction is adequate to produce the very high bicarbonate alkalinity observed within some of the monitoring zones (e.g. 522 mg/l; well 3). We also note that in several wells (Table 2) small concentrations of dissolved oxygen were detected with sulfide which indicates a lack of oxidation-reduction equilibrium.

The negative sodium and potassium ion deviations with respect to the conservative mixing line (Figures 5a and 5b) may have resulted from reverse ion exchange. This is a process in which aqueous monovalent ions are exchanged for divalent ions present on clay mineral surfaces prior to the introduction of seawater. Sayles and Manglesdorf (1977) have shown that a variety of clay minerals when introduced to seawater will exchange calcium from their surfaces for aqueous sodium. Potassium and magnesium concentrations undergo similar changes but to a smaller extent. The loss of sodium and the accompanying release of calcium is a possible factor responsible for the relatively rare calcium-chloride water type observed at well locations 7 and 11.

The zone of dispersion is considered an ideal setting for carbonate mineral dissolution because of the influx of high ionic strength, cool seawater (Plummer,1975 and Vernon,1969). Enhanced secondary porosity in the form of vugs, molds, and cavities was either directly observed in core samples or inferred from the loss of drilling fluids within the Pliocene-Miocene mixing zone. Calcium ion concentrations (Figure 5c) throughout the Pliocene-Miocene aquifer were greater than those which would result from the conservative mixing of seawater and a freshwater end-member. For these reasons carbonate dissolution must be considered as a possible control upon the groundwater chemistry of the confined aquifer system.

Sanford and Konikow (1989) have shown through a combined numerical flow simulation and chemical mass transport model that nearly all calcite dissolution will occur in the more dilute portion of the mixing zone (i.e. a few percent seawater). Interestingly, the most notable calcium ion deviations (Well 11; Figure 5c) with respect to the conservative mixing line occur at low seawater concentrations. Calcium ion concentrations were considerably lower in those well locations where the seawater concentration was greater than 5%. This trend is also consistent with the Sanford and Konikow (1989) model. The relatively high calcium ion concentrations observed in the dilute part of the mixing zone correspond to the negative sodium ion deviations. However, the positive calcium

ion deviations were approximately 10-20 times greater in terms of equivalents than the negative sodium ion deviations. Therefore, ion exchange is probably not responsible for most of the positive calcium ion deviation.

These deviations with respect to the mixing line are most likely the result of calcite dissolution. Unfortunately this cannot be rigorously demonstrated in that the calcite saturation indices (Table 2) within the mixing zone were typically greater than zero. Two complicating factors need be considered with respect to this apparent anomaly. One possibility is that that the partial pressure of carbon dioxide was locally greater witin organic-rich zones than those values derived from our measurements and calculations. Another complication involves the laboratory measurement of pH which results in calculated PCO_2 values which are lower than the ambient groundwater values. The pH measurements made in the field during the first sampling period were typically 0.2-0.5 units less than those measurements made during the second sampling period. However, the WATEQF-calculated saturation indices associated with the first sampling period, like those for the second sampling period, were mostly positive. Therefore, we have no direct evidence that groundwater in the mixing zone is undersaturated with respect to calcite (or dolomite). Thus the source of calcium and the observed positive deviations with respect to the conservative mixing line remain problematic.

SUMMARY AND CONCLUSIONS

The results of this investigation clearly indicate that modern saltwater is encroaching the confined aquifer system located in the southern portion of the island, close to a navigation channel. Although this relationship seems more than coincidental, we cannot definitively conclude that the dredging of the navigation channel is the source of saltwater. We observed brackish water (32% seawater) within the Miocene aquifer, well below the base of the channel and effectively confined from the overlying Pliocene-Miocene aquifer. We also noted that our one measurement of the potentiometric surface to date indicated that seawater may be originating from some natural offshore exposure. Limited carbon-14 data confirm the hypothesis that recent ocean water is mixing with older fresh groundwater. Unfortunately, detailed baseline (pre-dredging) hydrochemical data do not exist for the study area; therefore, the effects of dredging and other human manipulations cannot be unequivocally determined from this study.

The lithology of the Pliocene-Miocene confined aquifer underlying Cumberland Island and the related hydrochemical processes are remarkably variable and complex. Magnesium was the only major ion which mixed conservatively over the entire range of salinities (3-88% seawater). The most notable deviations occurred with respect to bicarbonate and calcium. Calcium ion concentrations were the highest in the dilute portion of the mixing zone. Local organic-rich zones were hypothesized to be an important feature controlling the aqueous geochemistry within the Pliocene-Miocene mixing zone. These zones were evidenced by the presence of anaerobic (and in some cases sulfidic) water in which sulfate reduction was inferred. Sulfate reduction is in turn responsible for the high alkalinity values observed at some sampling locations. The exchange of adsorbed calcium for aqueous sodium was hypothesized to explain negative

sodium ion deviations with respect to the freshwater-saltwater mixing line.

ACKNOWLEDGEMENTS

We gratefully acknowledge funding for this study which was provided by the National Park Service and the United States Geological Survey under the Cooperative Agreement CA 5000-5-8091 with Georgia State University.

REFERENCES CITED

Berner, E.K. and Berner, R.A., 1987, The Global Water Cycle: Prentice-Hall, Inc., Englewood Cliffs, New Jersey, 397 p.

Hanshaw, B.B., Back, W., Rubin, M., and Wait R.L., 1965, Relation of carbon 14 concentrations to saline water contamination of coastal aquifers: Water Resources Research, v.1, p. 109-114.

Hardie, L.A., 1987, Dolmitization: A critical view of some current views: Journal of sedimentary Petrology, v.57, p. 166-183.

Hanshaw, B.B., Back W., and Deike R.G., 1971, A geochemical hypothesis for dolomitization by ground water: Economic Geology, v.66, p. 710-724.

Harris, W.H., 1967, Stratification of fresh and salt water on barrier islands as a result of differences in sediment permeability: Water Resources Research, v.3, p. 89-97.

McLemore, W.H., Swann, C.T., Wigley P.B., Turlington, M.C., Henry, V.J., Nash, G.J., Martinez, J., Carver, R.E., Thurmond, J.T., 1981, Geology as applied to land-use management on Cumberland Island, Georgia: Georgia Geologic Survey, Atlanta, GA.

Plummer, L.N., 1975, Mixing of sea water with calcium carbonate ground water: *in* Geological Society of America Memoirs, v.142, Quantitative Studies in the Geological Sciences, Edited by E.H.T. Whitten, p. 219-236.

Plummer, L.N., Jones, B.F., and Truesdell, A.H., 1976, WATEQF - A FORTRAN IV version of WATEQ, A computer program for calculating chemical equilibrium of natural waters - user's guide: U.S. Geological Survey Water Resources Investigation 76-13.

Reilly, T.E. and Goodman, A.S., 1985, Quantitative analysis of saltwater-freshwater relationships in groundwater systems - A historical perspective: Journal of Hydrology, v.80, p. 125-160.

Sanford, W.E. and Konikow, L.F., 1989, Simulation of calcite dissolution and porosity changes in saltwater mixing zones in coastal aquifers: Water Resources Research, v.25, p. 655-667.

Sayles, F.L. and Mangelsdorf, P.C., 1977, The equilibration of clay minerals with seawater: exchange reactions: Geochimica et Cosmochimica Acta, v.41, p. 951-960.

Stoessel, R.K., Ward, W.C., Ford, B.H., and Schuffert, J.D., 1989, Water chemistry and CaCO3 dissolution in the saline part of an open-flow mixing zone, coastal Yucatan Peninsula, Mexico: Geological Society of America Bulletin, v.101, p. 159-169.

Vacher, H.L., 1978, Hydrogeology of Bermuda - Significance of an across-the-

island variation in permeability: Journal of Hydrology, v.39, p. 207-226.
Vernon, R.O., 1969, The geology and hydrology associated with a zone of high permeability (boulder zone) in Florida: Society of Mining Engineers, Preprint 69-AG-12, 24 p.
Wilson, S.K., 1990, The hydrogeochemistry of southern Cumberland Island, Georgia. Unpublished M.S. thesis, Georgia State University, Atlanta, GA., 81 p.

STRUCTURE AND CHRONOLOGY OF PART OF THE PENNYRILE FAULT SYSTEM, WESTERN KENTUCKY

D. K. LUMM
W. J. NELSON

Illinois State Geological Survey
615 East Peabody Drive
Champaign, IL 61820

S. F. GREB

Kentucky Geological Survey
Lexington, KY 40506

ABSTRACT

Geologic mapping of railroad and highway cuts north of Crofton, Kentucky, suggests that Cambrian normal faults of the Pennyrile Fault System were reactivated during Morrowan and Atokan (Pennsylvanian) time, triggering slump faults and producing angular unconformities in the Caseyville and Tradewater Formations. Angular unconformities in the lower part of the Tradewater Formation suggest that minor uplift was contemporaneous with sedimentation. Major offset across the fault zone is normal and down to the north, and occurred after deposition of the Tradewater Formation. Minor folds and overthrusts indicate that regional north-south extension was followed by localized compression within the fault zone. Interpretations of movement along the fault zone during Morrowan and Atokan time differ from previous reports that describe only late-or post-Pennsylvanian movement.

INTRODUCTION

The Pennyrile Fault System is a 100-mile-long (162 km) east-west trending network of en echelon faults located in western Kentucky (Figure 1). The faults are predominantly high-angle normal, but reverse, thrust, and strike-slip faults at some locations have been reported by Jillson (1958), Rose (1963), and Lee Higgins (personal communication, 1988). The fault system forms part of the southern boundary of the coal-bearing Eastern Interior (Illinois) Basin and of the smaller Moorman Syncline. The composite displacement of the Mississippian and Pennsylvanian surface rocks is normal and down to the north. Displacement on the fault system diminishes eastward and terminates on the western flank of the Cincinnati Arch. The displacement across individual faults increases westward to a maximum of approximately 800 ft (245 m) near Crofton, Christian County, Kentucky. About 30 miles (50 km) west of Crofton the Pennyrile Fault System bends to the southwest and projects into the Mississippi Embayment. In this area the faults are concealed by undisturbed Late Cretaceous (Gulfian) sediments and may merge with the northeast-trending Fluorspar Area Fault Complex beneath the embayment sediments. The age of faulting for the Pennyrile Fault System is reported to be post-Desmoinesian (middle Pennsylvanian) to pre-Late Cretaceous

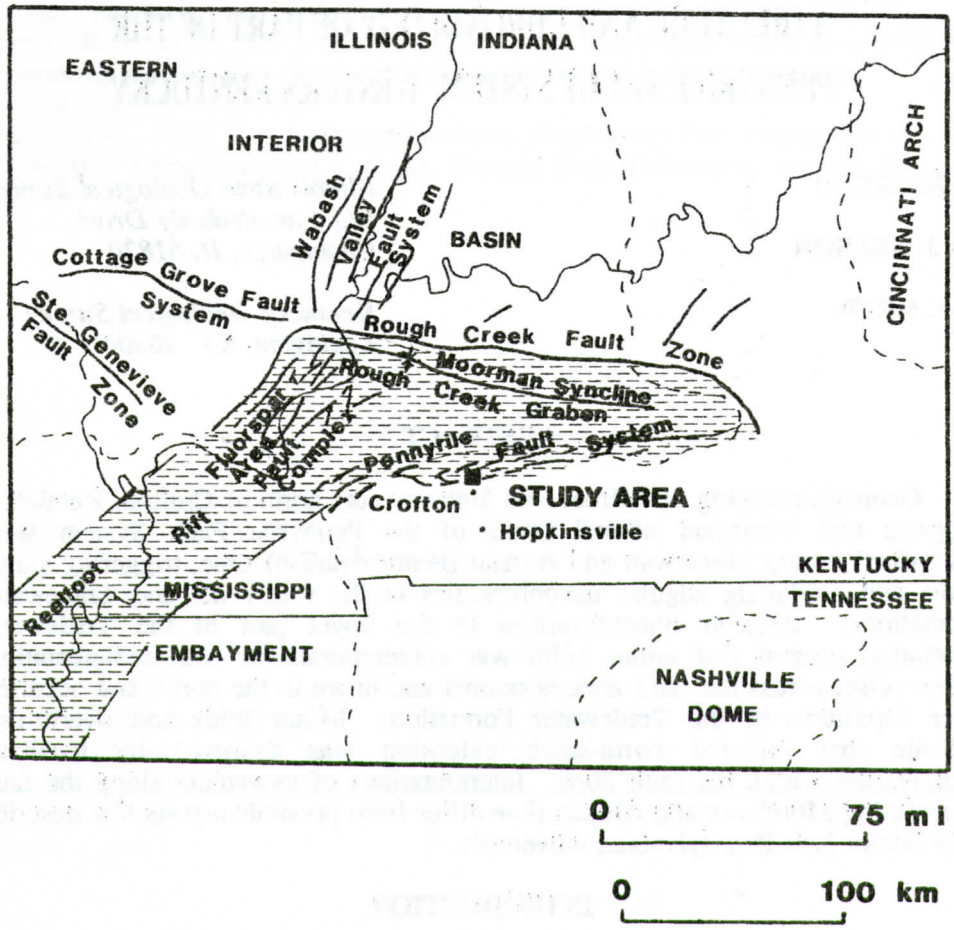

Figure 1. Location map showing the study area and the Pennyrile Fault System, Rough Creek Fault Zone, Rough Creek Graben, and other structures in the western Kentucky region. Stippled area represents Cambrian rift basin.

by Nelson and Lumm (1984) based on the displacement of Desmoinesian strata.

Recent subsurface and geophysical studies have determined that the Pennyrile Fault System is approximately coincident with the southern margin of a deep subsurface structure known as the Rough Creek Graben (Soderberg and Keller, 1981; Lumm, 1988; Lumm and Stearns, 1989). The graben is continuous with and genetically related to the Reelfoot Rift, a Late Precambrian to Early Cambrian aulacogen (Schwalb, 1982). Proprietary seismic reflection profiles verify that the Pennyrile Fault System is composed of north-dipping normal faults that penetrate Precambrian crystalline basement. Cambrian strata thicken substantially in downthrown fault blocks, indicating fault displacement during the Cambrian Period. Intermittent growth faulting from Upper Cambrian to Devonian time is indicated by thickening of stratigraphic units within the Rough Creek Graben north of the Pennyrile Fault System (Schwalb, 1982; Buschbach and

Schwalb, 1984).

Gravity profiles across the Pennyrile Fault System north of Crofton indicate overthickened Pennsylvanian sediments and possible faulting during the deposition of these sediments (Lumm, 1988). Tectonic influences on Pennsylvanian sedimentation have been reported in other areas related to the Rough Creek Graben from scattered outcrops or subsurface data (Potter, 1957; Amos, 1966; Shawe and Gildersleeve, 1969; Davis and others, 1974; Mathis, 1983; Neuder, 1984; Nelson and Lumm, 1984 and 1985; Greb, 1989a and b; C. Pius Weibel, personal communication, 1988).

This paper describes the structure and chronology along a portion of the Pennyrile Fault System north of Crofton, Kentucky. In that area, faults and fault-controlled sedimentary units can be recognized in excellent exposures within a railroad cut and in a parallel highway cut 1.2 miles (2 km) to the east. Both cuts provide almost continuous profiles of the fault zone. The structural detail visible in the railroad cut is unrivaled elsewhere in the Eastern Interior Basin. These exposures previously have been cited as evidence of normal and reverse movement. Kehn (1977) mapped three faults crossing the railroad and highway cuts but did not discuss their detailed characteristics or chronology. Whaley and others (1979) described some of the structures in the Pennyrile Parkway roadcuts but did not discuss chronological relationships.

This study will show evidence for three episodes of down-to-the-north normal faulting and for tectonic influences on sedimentation. In addition, reverse faults with offsets of less than 3 ft (1 m), strike-slip faults, and folds indicate final adjustment of fault blocks by localized compression. Our conclusions differ from previous field studies of the Pennyrile Fault System that have suggested either a simple history or one involving major reverse or strike-slip movement (Jillson, 1958; Rose, 1963; Lee Higgins, written communication to W. J. Nelson, 1988).

Data and Location of Study

Data for this study consists of outcrop mapping of strata exposed in a railroad cut and parallel highway cuts approximately 1 mile (1.6 km) north of Crofton, Kentucky (Figure 2). One of the localities is the 4,500 ft long (1,370 m) CSX Railroad cut. The other locality includes two roadcuts made for the multilane Pennyrile Parkway, located 1.2 miles (2 km) east of the railroad cut. The roadcuts, each approximately 1000 ft (300 m) long are separated by a fill 300 ft (90 m) long, and maximum height of exposure in the railroad and highway cuts is about 70 ft (21 m).

Stratigraphy

The stratigraphic units exposed in the railroad and highway cuts are graphically represented in Figure 3. The vertical succession in the cuts includes the Menard Limestone (oldest), Palestine Formation, Degonia Formation and Kinkaid Limestone of the Chesterian Series, and the Caseyville and Tradewater Formations of the Morrowan and Atokan Series. The Clore Formation, which normally occurs between the Palestine and Degonia, is faulted out of the succes-

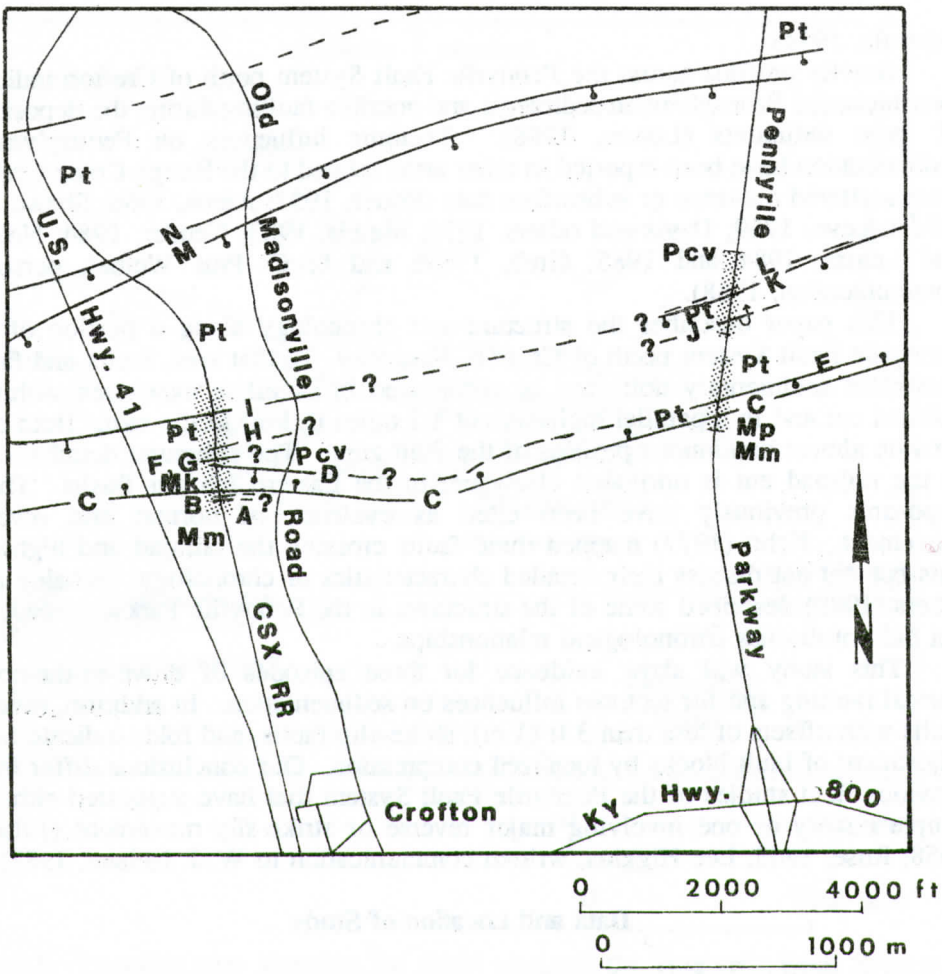

Figure 2. Map of the study area. Shaded areas indicate railroad and highway cuts. Faults labeled "A" through "M" are described sequentially in the text. Stratigraphic formations are abbreviated "Mm" for Menard Limestone, "Mk" for Kinkaid Limestone, "Pcv" for Caseyville Formation, "Pt" for Tradewater Formation, and are illustrated in Figure 3.

sion in the railroad cut. The Degonia, Clore, and Kinkaid are faulted out in the southern highway cut.

Our stratigraphic designation of rocks in the cuts differs somewhat from Kehn (1977) who mapped only the Menard Limestone and Caseyville Formation in these outcrops. The small map scale (1:24,000) probably precluded Kehn (1977) from mapping the narrow fault slices of Palestine, Degonia, and Kinkaid Formations recognized here. Also, Kehn (1977) mapped all Pennsylvanian rocks in these exposures as Caseyville Formation. Whaley and others (1979) followed Kehn's mapping. Our assignment of some Pennsylvanian rocks to the Tradewater Forma-

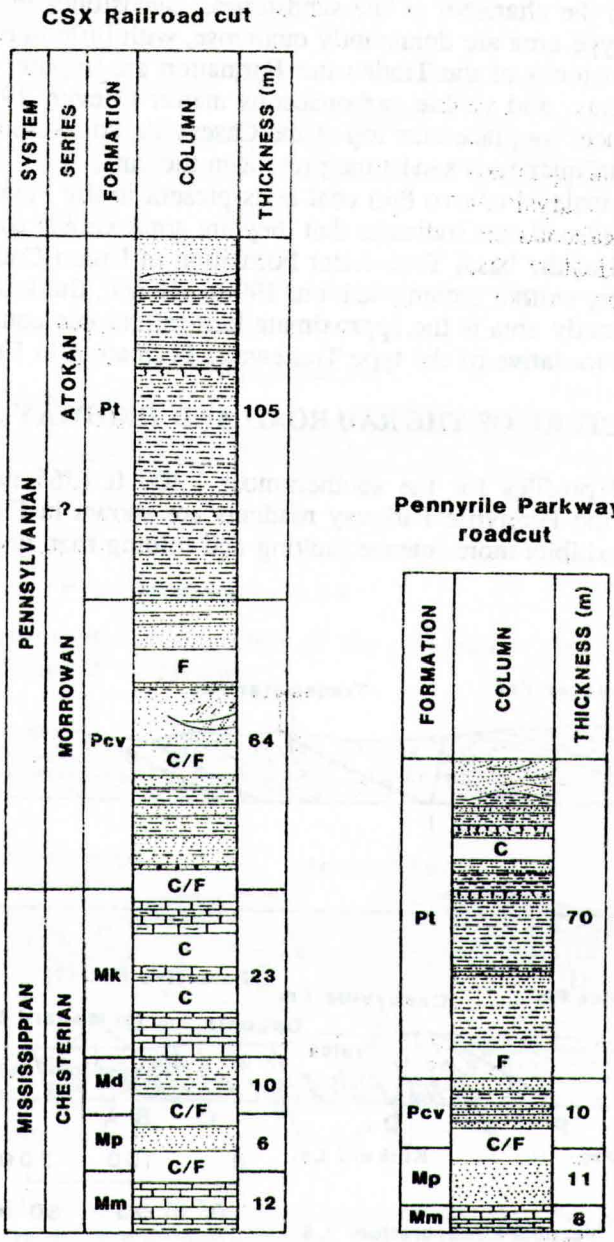

Figure 3. Stratigraphic columns of the rocks exposed in the CSX Railroad cut and in the Pennyrile Parkway roadcuts. LEGEND: Mm = Menard Limestone, Mp = Palestine Formation, Md = Degonia Formation, Mk = Kinkaid Limestone, Pcv = Caseyville Formation, Pt = Tradewater Formation, C = covered interval, F = faulted interval. The Clore Formation, which normally occurs between the Palestine Formation and the Degonia Formation, is faulted out of the succession in both locations.

tion is based upon the character of the sandstones. Sandstones in the Caseyville Formation in the type area are dominantly quartzose, with little mica or interstitial clay, whereas sandstones of the Tradewater Formation are impure, with abundant mica, interstitial clay, and visible carbonaceous matter (Siever, 1957; Potter and Glass, 1958). Hence, we placed the top of the Caseyville Formation at the highest occurrence of clean quartzose sandstone present in the cuts.

Palynologic analysis of two thin coal beds present in the Pennyrile Parkway and in the CSX Railroad cuts indicates that they are approximate correlatives with the Bell Coal Bed of the basal Tradewater Formation in Union County, Kentucky (Russel A. Peppers, written communication, 1990). Hence, the lower Tradewater Formation in the study area is the approximate biostratigraphic equivalent as well as the lithologic correlative of the type Tradewater Formation in Union County.

STRUCTURE OF THE RAILROAD AND HIGHWAY CUTS

Longitudinal profiles for the southernmost 1,200 ft (365 m) of the CSX Railroad cut and the Pennyrile Parkway roadcuts are shown in Figures 4 and 5. The railroad cut exhibits more intense faulting and folding than do the roadcuts.

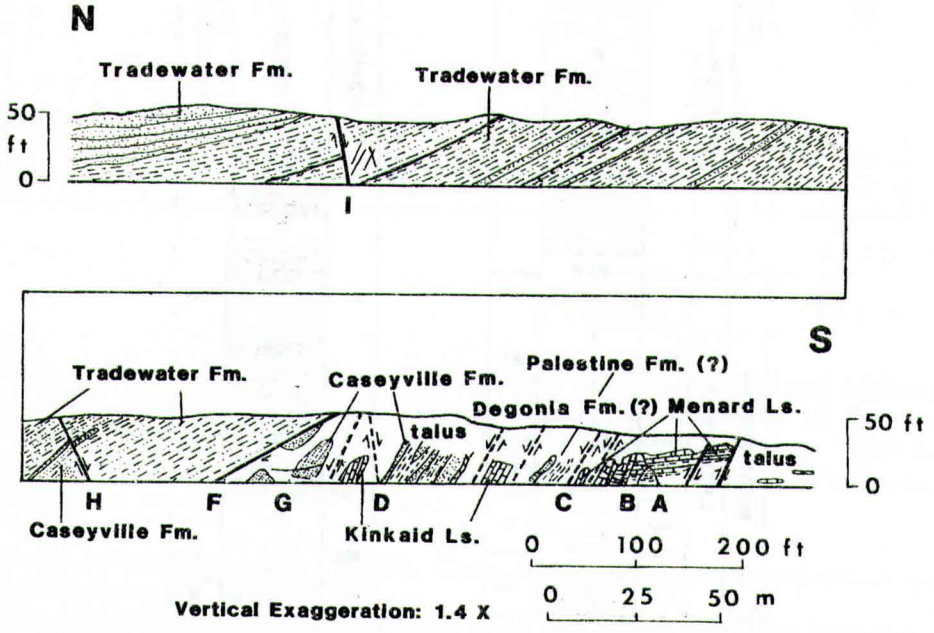

Figure 4. Diagrammatic cross section of the east wall of the CSX Railroad cut. See Figure 2 for location.

The basic feature of the fault system north of Crofton is an asymmetrical graben defined by faults C and N on Figure 2. This feature widens eastward from about 4,000 ft (1,220 m) along the railroad track to about 5,000 ft (1,525 m) along the highway. Only one fault (fault C in Figure 2) can be directly traced between

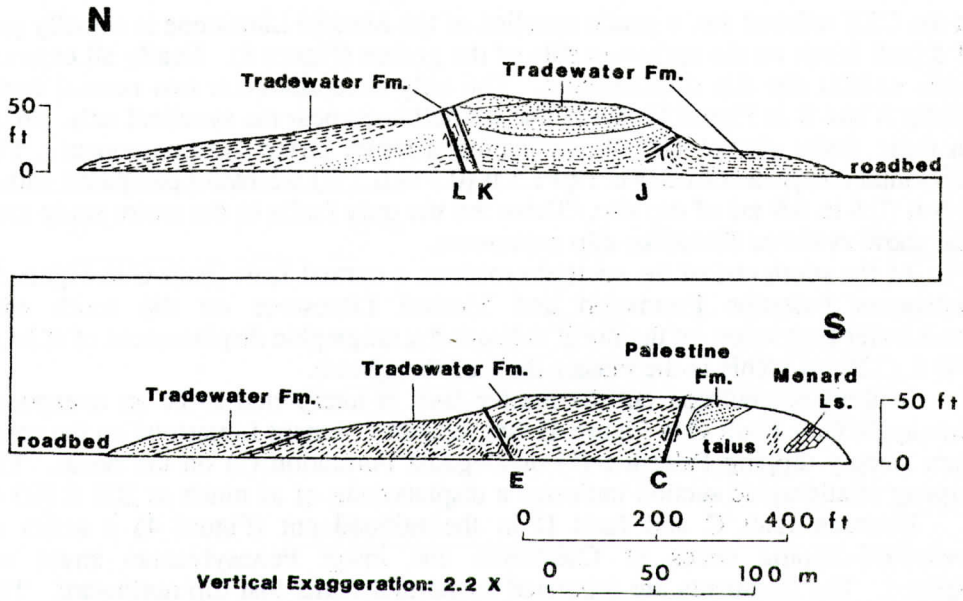

Figure 5. Diagrammatic cross section of the east wall of the Pennyrile Parkway roadcuts. See Figure 2 for location.

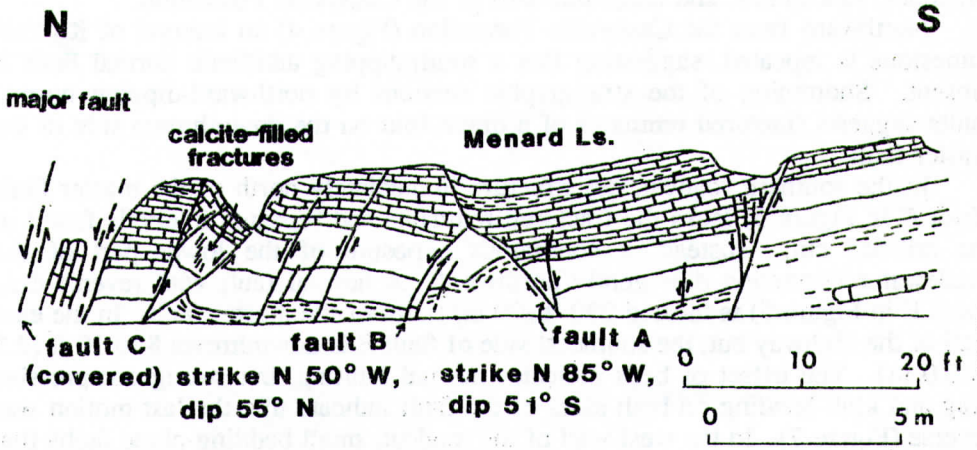

Figure 6. A gentle syncline in Menard Limestone showing faults A, B, and C in the east wall of the CSX Railroad cut. See Figure 4 for location.

the cuts. Fault D (unexposed) at the railroad cut, may be continuous with fault E of the southern highway roadcut. Fault I of the railroad cut may bifurcate and connect with faults K and L in the northern roadcut. Faults N and M in the railroad cut most likely connect with faults located in a third highway cut located north of faults K and L (Figure 2).

South of all major faults, poorly exposed Menard Limestone dips 5-10°N.

In the CSX railroad cut, a gentle syncline of the Menard Limestone is actually part of a fault block on the upthrown side of the graben (Figure 6). Nearly all exposed faults exhibit dip slip displacement. The only exceptions are two normal faults (faults A and B in Figure 6) that bound a small horst near the synclinal axis. Striae on these faults plunge 60° W, indicating a minor strike-slip component. The horizontal component of slip is 1 to 1.5 ft (0.3 to 0.5 m) westward compared with 2 to 3 ft (0.6 to 0.9 m) of dip slip. These are the only faults in the entire study area that show evidence for strike-slip movement.

At the south end of the southern roadcut, a normal fault (fault C in Figure 5) juxtaposes Palestine Formation and Menard Limestone on the south with Tradewater Formation on the north indicating stratigraphic displacement of at least 400 ft (120 m). This is the master fault of the system.

In the CSX railroad cut the master fault is interpreted to be an unexposed high-angle fault (fault C in Figure 4) that separates Menard Limestone on the south from steeply dipping Palestine (?) or Degonia Formation (?) on the north. The missing stratigraphic section indicates a displacement of as much as 200 ft (60 m).

Between fault C and fault D in the railroad cut (Figure 4) a series of northward-dipping slices of Chesterian and lower Pennsylvanian strata are exposed. The fragments are separated by normal faults that dip northward. The succession, from south to north, begins with approximately 30 ft (9 m) of Palestine or Degonia Formation strata. These beds are juxtaposed against an intensely fractured block of Kinkaid Limestone. Further north in the railroad cut are siltstones, sandstones, and conglomerates of the Caseyville Formation.

Northward from the Caseyville Formation (Figure 4) an interval of Kinkaid Limestone is repeated, suggesting that a south-dipping antithetic normal fault is present. Shortening of the stratigraphic sections by northward-dipping normal faults suggests fractured remnants of a drape fold on the downthrown side of the master fault.

In the southern roadcut, the structure immediately north of the master fault (fault C in Figure 5) lacks the fractured remnants and repeated intervals found in the railroad cut. Instead, a continuous exposure of the lower part of the Tradewater Formation dips gently northward. A normal fault with reverse drag (fault E in Figure 5) is located 230 ft (70 m) north of the master fault. In the east wall of the highway cut, the southeast side of fault E is downthrown 8 to 10 ft (2.5 to 3.0 m). The offset of beds indicates normal faulting, but strong compressive drag and kink-banding on both sides of the fault indicate that the last motion was reverse (Figure 7). In the west wall of the roadcut, small bedding-plane faults that may represent flexural slip, offset the high-angle fault E (Figure 8). These relationships indicate at least three increments of movement at this locality; that is, normal faulting was followed in turn by reverse movement and then by bedding plane slip.

Some of the most complex and informative structural relationships are found in the railroad cut between faults D and F (Figures 4 and 9). Fault F in Figure 9 exhibits faulted Pennsylvanian strata in which the fault is subparallel to the bedding of both the footwall and the hanging wall. Just below this fault is a lozenge-shaped block of very fine-grained sandstone that overlies dark gray shale and thin-to thick-bedded sandstone. Above fault F are silty shales and siltstones.

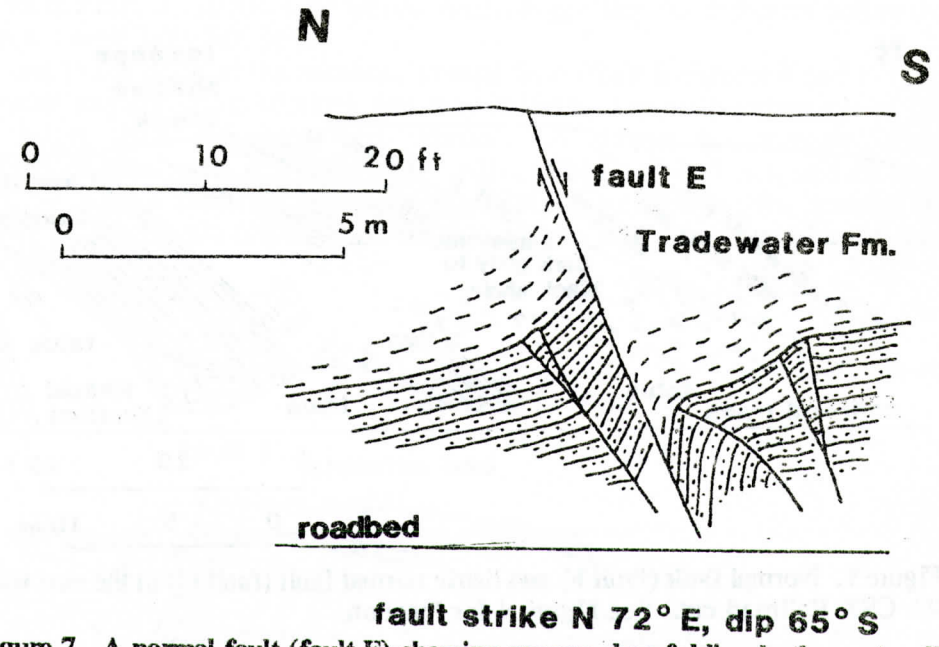

Figure 7. A normal fault (fault E) showing reverse drag folding in the east wall of the southern Pennyrile Parkway roadcut. See Figure 5 for location.

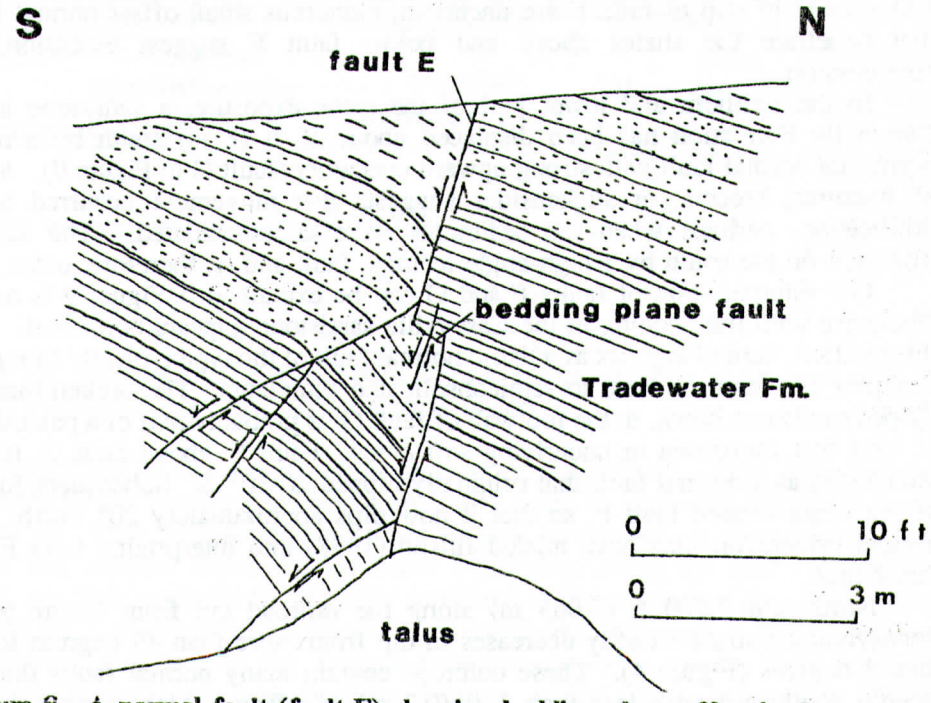

Figure 8. A normal fault (fault E) showing bedding plane offset in the west wall of the southern Pennyrile Parkway roadcut. See Figure 5 for location.

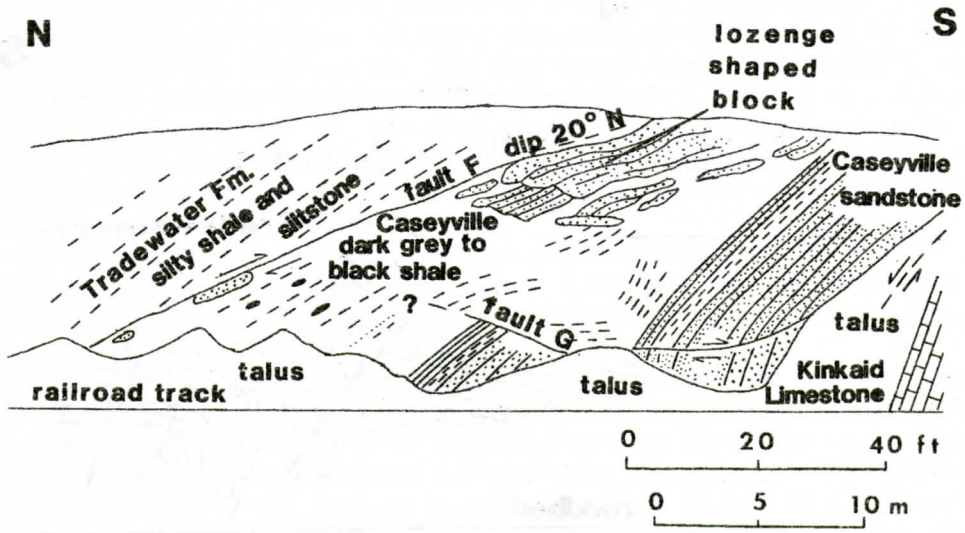

Figure 9. Normal fault (fault F) and listric normal fault (fault G) in the east wall of the CSX Railroad cut. See Figure 4 for location.

Jillson (1958) interpreted fault F as a thrust fault, and thereby inferred an important element of compression in the Pennyrile Fault System. Although the direction and amount of slip of fault F are uncertain, numerous small-offset normal faults that penetrate the shales above and below fault F suggest extension, not compression.

In the southern and lower part of the same exposure, a sandstone in the Caseyville Formation has been displaced about 25 ft (8 m) south by a nearly horizontal normal fault with strong upward concavity (fault G in Figure 9). A lack of fractures, breccia, or slickensides suggests that movement occurred before lithification, perhaps when the sediments were unconsolidated. The fault is truncated on the south by a high-angle tectonic fault and is, therefore, older.

Our interpretation of faults F and G can be explained if Figure 9 is rotated clockwise until the bedding in the Caseyville sandstone appears horizontal. With this rotation, fault G appears as a listric normal fault of the type typically formed by slumping of unconsolidated to semiconsolidated sediments. The broken lozenge-shaped sandstone block, in the footwall of fault G, is probably part of a paleoslump of sand that foundered in underlying soft muds. Fault F, above fault G, is here interpreted as a normal fault that originally dipped 20-30° S. Subsequent folding of the strata rotated fault F, so that it now dips approximately 20° north. The present orientation may have misled Jillson (1958) into interpreting fault F as a thrust fault.

Northward 3,500 ft (1,065 m) along the railroad cut from Figure 9, the Pennsylvanian strata steadily decreases in dip from more than 45 degrees to less than 3 degrees (Figure 4). These outcrops contain many normal faults that dip steeply southward with less than 1 ft (0.3 m) of offset. Also, a normal fault antithetic to the master fault of the system (fault H in Figure 4) displaces a 4 ft

thick (1.2 m) sandstone approximately 90 ft (27 m) down to the south. The fault exhibits no drag, slickensides, or breccia clasts, suggesting that it formed before the sediments were fully lithified.

Just to the north of the antithetic normal fault (fault I; Figures 4 and 10) are two small angular unconformities that may indicate very early movement of the fault before these sediments were lithified. A siderite bed truncates tilted siltstones of the Tradewater Formation. Also, a thin coal bed truncates its own underclay and the subjacent sandstone and siltstone. Although these features do not indicate large-scale displacement they do suggest small movements at the time of deposition.

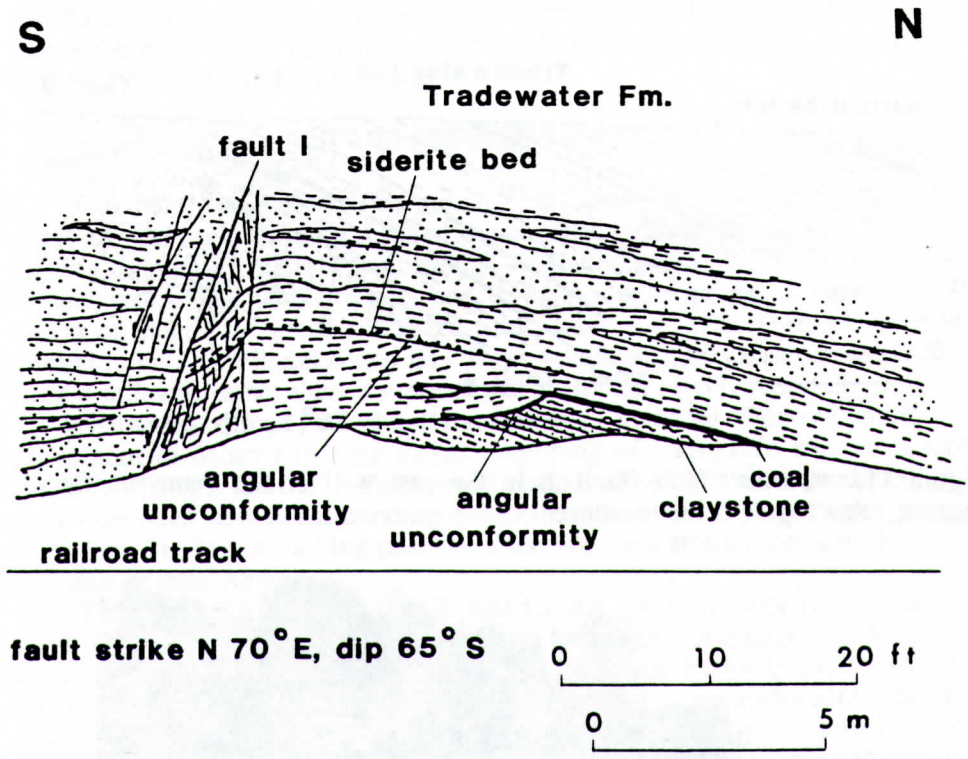

Figure 10. Normal fault (fault I) with angular unconformities in the west wall of the CSX Railroad cut. See Figure 4 for location.

About 200 ft (60 m) north of the angular unconformities, a thick cross-bedded sandstone in the Tradewater Formation shows north to northeast-dipping foresets (Figure 4). Thin, sheet-like sandstones thicken northward on downthrown fault blocks and indicate movement or minor subsidence along the faults. North of fault I, multiple channels sequentially truncated to the north (not shown in Figure 4) indicate a northward migration of minor fluvial channels. The northward paleocurrent direction of this channel-facies sandstone is nearly 180° from the dominant regional average direction (Potter, 1957; Davis and others, 1974; Whaley and others, 1979; Greb, 1989a), and coincident with the direction of

downthrow on fault I.

Evidence for localized compressional deformation is shown in Tradewater strata in the northern highway cut (fault J in Figures 5 and 11). A thrust-faulted and overturned asymmetric anticline of sandstone, siltstone, and a coal bed that is the approximate correlative of the Bell Coal Bed of the Tradewater Formation show low-angle kink banding in strata of the overturned limb of the fold.

A 28-ft wide (9 m) fault block of thoroughly fractured, pebbly quartz arenite of the Caseyville Formation is bounded by faults K and L (Figures 5 and 12).

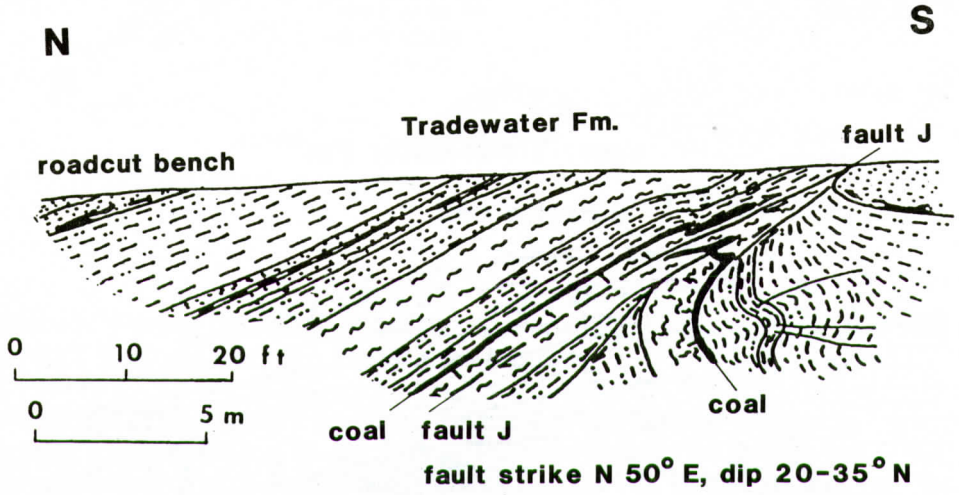

Figure 11. "Thrust" fault (fault J) in the east wall of the Pennyrile Parkway roadcut. See Figure 5 for location.

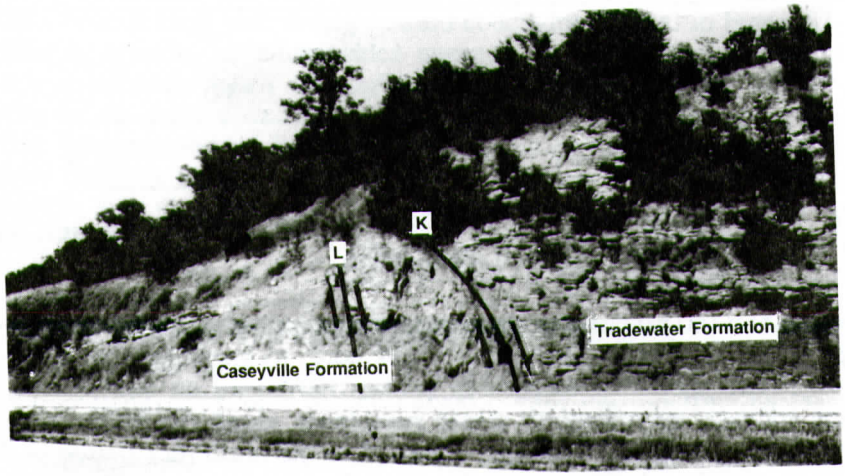

Figure 12. Fault block of Caseyville Formation bounded by high angle faults (faults K and L) in the east wall of the Pennyrile Parkway roadcut. See Figure 5 for location.

The fault block is wedged between a gently dipping block of sandstone and siltstone (Tradewater Formation) to the south and a north-dipping sandstone section of the Caseyville Formation on the north. Bedding in this central block indicates normal movement with an estimated total displacement of 200 ft (60 m). If faults K and L were projected into the subsurface, they would intersect the north-dipping master fault, fault C, in Mississippian strata approximately 1,400 ft (425 m) below the level of the roadway. The intersection of these structures would form an asymmetrical graben.

A similar graben structure about 4,000 ft (1,220 m) wide can be reconstructed by projecting southward dipping faults M and N (Figure 2) into the subsurface to an intersection with fault C. Both faults M and N have displacements of about 500 ft (150 m) and would intersect fault C in Ordovician strata about 5,000 ft (1,525 m) below the level of the roadway. These grabens are the principal structures of this part of the Pennyrile Fault System.

SUMMARY AND DISCUSSION

Our field data indicate that the major structure of the Pennyrile Fault System north of Crofton, Kentucky is an asymmetric graben, dominated by a north-dipping, high-angle normal fault (fault C). The magnitude of the principal dip-slip normal faults (e.g., faults C, K, and L) have displacements approximately two orders of magnitude greater than the thrust fault (e.g., fault J) or the oblique-slip normal faults (e.g., faults A and B). These relations signify that extensional events were dominant, rather than compressional as Jillson (1958) reported.

At least three periods of movement involved Pennsylvanian strata. Movement in Morrowan time caused slumping of Caseyville sediments along a listric fault (e.g., fault G). The second episode in Atokan time produced angular unconformities and north-trending paleocurrents in lower Tradewater sediments (e.g., fault I). Major faulting post-dates the youngest strata present in the outcrops and thus is post-Atokan.

The antithetic faults (faults K and L) and the north-dipping synthetic fault (fault C) outline a graben several thousand feet wide and mapped by Kehn (1977) for thousands of feet beyond the CSX and Pennyrile Parkway exposures. In the study area the overall stratigraphic offset of Pennsylvanian rocks across the graben is approximately 800 ft (245 m). In the subsurface, the displacement increases to 1,200 ft (365 m) at the level of the New Albany Shale (Devonian-Mississippian; Schwalb and Potter, 1978). Collinson and others (1988) have approximated 5,000 ft (1,500 m) of basement offset in a 10 mile (6 km) wide north-south zone in the Crofton area. This increase in stratigraphic displacement at depth indicates that growth faulting occurred intermittently throughout much of Paleozoic time along the southern margin of the Rough Creek Graben.

The Pennyrile Fault System thus represents the Morrowan and later reactivation of basement faults along the southern margin of the Rough Creek Graben. A schematic diagram indicates the probable sequence of deformational events from Morrowan through post-Atokan times (Figure 13). Regional N-S to NW-SE horizontal extension in early Pennsylvanian time induced normal movement at depth on the north-dipping master fault, which was inherited from

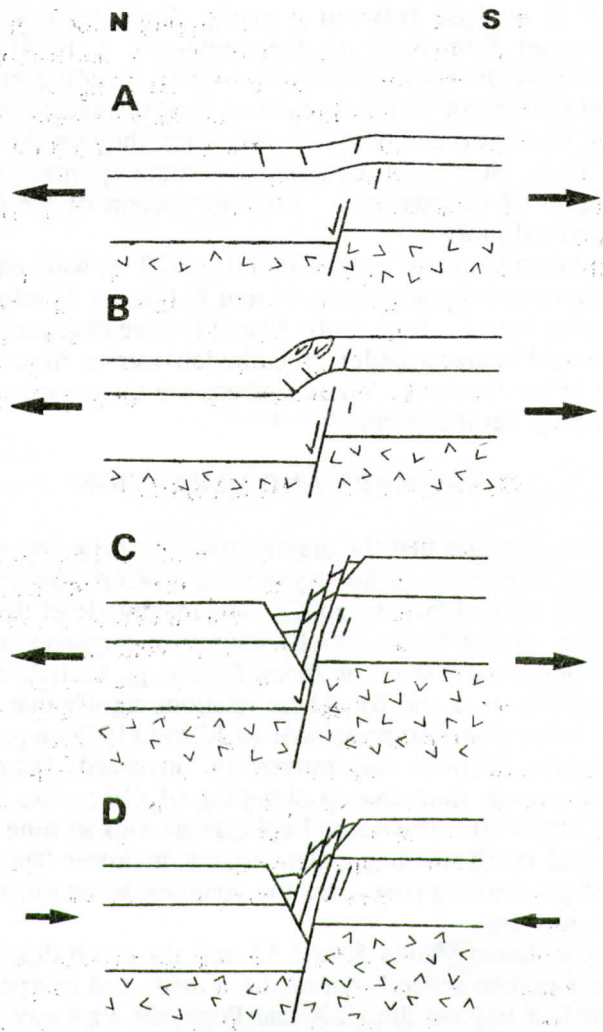

Figure 13. Schematic diagram summarizing history of development of Pennyrile Fault System in the study area. Arrows indicate vector magnitude and direction. (A) Early Pennsylvanian extension. (B) Near-surface strata deform in ductile fashion, initiating slumping and minor unconformities. (C) With continued extension, master fault reaches surface; antithetic faults develop. (D) Localized compression produces small thrust faults.

Cambrian rifting (Figure 13A). The near-surface rocks may have initially responded in a ductile fashion and a north-facing monoclinal drape fold formed, perhaps initiating slumping and minor unconformities of Caseyville and Tradewater sediments (Figure 13B). Under continued extension the master fault propagated to the surface, and south-dipping antithetic faults developed (Figure 13C). With continued extension and downward displacement, the fault blocks near the master fault rotated northward and earlier-formed faults, such as the listric

faults in the railroad cut, were themselves rotated. As rotation continued, the rocks were folded and flexural-slip faults developed along bedding planes. Localized north-south compression within the graben produced small thrust faults, high-angle reverse faults, and kink bands, probably due to downward wedging of the blocks as the graben was formed (Figure 13 D). Strike-slip movement along fault blocks is a probably the result of local shearing and final adjustment of fault blocks.

Our interpretation of Morrowan and Atokan syndepositional movement along faults and associated controls on sedimentation complements interpretations of early Pennsylvanian structural activity in other parts of the Eastern Interior Basin (Potter, 1957; Amos, 1966; Shawe and Gildersleeve, 1969; Davis and others, 1974; Nelson and Lumm, 1985; Greb, 1989a and b; and Weibel and others, in press), as well as the movement along the Alleghanian orogeny in the Appalachian Basin (Dean and others, 1988; Ferm and Weisenfluh, 1989; Greb and others, 1990; Chesnut, 1991).

REFERENCES

Amos, D. H., 1966, Geologic map of the Golconda and Brownfield Quadrangles, Livingston County, Kentucky: U.S. Geological Survey GQ-546, scale 1:62,500.

Buschbach, T. C., and Schwalb, H. R., 1984, Sedimentary geology of the New Madrid Seismic Zone, *in* Gori, P. L., and Hayes, W. W., eds., Proceedings of the symposium on the New Madrid Seismic Zone: U.S. Geological Survey, Open File Report 84-770, p. 64-96.

Chesnut, D. R., 1991, Timing of Alleghanian tectonics determined by Central Appalachian foreland basin analysis: Southeastern Geology, v. 31, no. 4.

Collinson, C. C., Sargent, M. L., and Jennings, J. R., 1988, *in* Sloss, L. L., ed., Sedimentary cover-North American craton U.S.: Geological Society of America, The geology of North America, v. D-2, Fig. 6.

Davis, R. W., Plebuch, R. O., and Whitman, H. M., 1974, Hydrology and geology of deep sandstone aquifers of Pennsylvanian age in part of the Western Coal Field region, Kentucky: Kentucky Geological Survey, Series X, Report of Investigations 15, 26 p.

Dean, S. L., Kulander, B. R., and Skinner, J. M., 1988, Structural chronology of the Alleghanian orogeny in southeastern West Virginia: Geological Society of America Bulletin, v. 100, p. 299-310.

Ferm, J. C., and Weisenfluh, G. A., 1989, Evolution of some depositional models in Late Carboniferous rocks of the Appalachian coal fields: International Journal of Coal Geology, v. 12, p. 259-292.

Greb, S. F., 1989a, A sub-rectangular paleovalley system, Caseyville Formation, Eastern Interior Basin, western Kentucky: Southeastern Geology, v. 30, no. 1, p. 59-75.

Greb, S. F., 1989b, Paleoslump along the upland unconformity surface, *in* Cecil, C. B. and Eble, C., eds., Carboniferous geology of the Eastern United States: American Geophysical Union, 28th International Geological Congress, Guidebook T143, p. 44-47.

Greb, S. F., Chesnut, D. R., Davidson, O. B., and Rodriguez, R., 1990, Mass flow deposits in the Lee Formation, eastern Kentucky coal field: Southeastern Geology, v. 31, no. 2, p. 79-91.
Jillson, W. R., 1958, Geology of the White Thorn Fault in northern Christian County, Kentucky: Frankfort, Kentucky, Perry Publishing Co., 16 p.
Kehn, T. M., 1977, Geologic map of the Crofton Quadrangle, Christian and Hopkins Counties, Kentucky: U.S. Geological Survey GQ-1361, scale 1:24,000.
Lumm, D. K., 1988, Gravity anomalies of the western portion of the Pennyrile Fault System and Rough Creek Graben, western Kentucky: Nashville, Tennessee, Vanderbilt University, unpublished M.S. Thesis, 155 p.
Lumm, D. K., and Stearns, R. G., 1989, Gravity anomalies of the southern branch of the Pennyrile Fault System and Rough Creek Graben, western Kentucky: Geological Society of America, North-Central Meeting, Abstracts with Programs, v. 21, no. 4, p. 40.
Mathis, H., Jr., 1983, Structural and sedimentological study of the accumulation of the No. 9 Coal to No. 13 coal zone interval in the western Kentucky Coal field: Lexington, University of Kentucky, unpublished M.S. Thesis, 103 p.
Nelson, W. J., and Lumm, D. K., 1984, Structural geology of southeastern Illinois and vicinity: Illinois State Geological Survey, Contract/Grant report 1984-2, 127 p.
Nelson, W. J., and Lumm, D. K., 1985, Ste. Genevieve Fault Zone, Missouri and Illinois: Illinois State Geological Survey, Contract/Grant report 1985-3, 94 p.
Neuder, G. L., 1984, Controls on peat accumulation in the No. 9 to No. 13 coal interval in western Kentucky: Lexington, University of Kentucky, unpublished M.S. Thesis, 80 p.
Potter, P. E., and Glass, H. D., 1958, Petrology and sedimentation of the Pennsylvanian sediments in southern Illinois--A vertical profile: Illinois State Geological Survey, Report of Investigations 204, 60 p.
Potter, P. E., 1957, Breccia and small-scale Lower Pennsylvanian overthrusting in southern Illinois: American Association of Petroleum Geologists Bulletin, v. 41, no. 12, p. 2695-2709.
Rose, W. D., 1963, Oil and gas geology of Muhlenberg County, Kentucky: Kentucky Geological Survey, Series X, Bulletin 1, 118 p.
Schwalb, H. R., and Potter, P. E., 1978, Structure and isopach map of the New Albany-Chattanooga-Ohio Shale (Devonian and Mississippian) in Kentucky: Kentucky Geological Survey, Series X, scale 1:250,000.
Schwalb, H. R., 1982, Paleozoic geology of the New Madrid area: U.S. Nuclear Regulatory Commission, NUREG CR-2909, 61 p.
Siever, R. A., 1957, Pennsylvanian sandstones of the Eastern Interior Coal Basin: Journal of Sedimentary Petrology, v. 27, no. 3, p. 227-250.
Shawe, F. R., and Gildersleeve, B., 1969, Anastomosing channel complex at the base of the Pennsylvanian System in western Kentucky: U.S. Geological Survey Professional Paper 650-D, p. D206-D209.
Soderberg, R. K., and Keller, G. R., 1981, Geophysical evidence for deep basin in western Kentucky: American Association of Petroleum Geologists, v. 65,

no. 2, 226-234.
Whaley, P. A., Hester, N. C., Williamson, A. D., Pryor, W. A., and Potter, P. E., 1979, Depositional environments of Pennsylvanian rocks in western Kentucky: Kentucky Geological Survey, Annual Field Conference of the Geological Society of Kentucky, 1979, 48 p.